MSc Program
Environmental Technology & International Affairs

The urban heat island effect in courtyards: A microclimatic analysis of courtyards in Vienna

A Master's Thesis submitted for the degree of
"Master of Science"

supervised by
Univ.Prof. Dipl.-Ing. Dr.techn. Ardeshir Mahdavi

Laura Glasberg

0703605

Vienna, 21.10.2015

Affidavit

I, **Laura Glasberg**, hereby declare

1. that I am the sole author of the present Master's Thesis, "THE URBAN HEAT ISLAND EFFECT IN COURTYARDS: A MICROCLIMATIC ANALYSIS OF COURTYARDS IN VIENNA", 70 pages, bound, and that I have not used any source or tool other than those referenced or any other illicit aid or tool, and
2. that I have not prior to this date submitted this Master's Thesis as an examination paper in any form in Austria or abroad.

Vienna, 21.10.2015

_____

Signature

Abstract

The urban heat island phenomenon was proven to have negative economic and health consequences on urban populations and is hence one of the most important climatic issues to be dealt with in the 21st century. This paper aims at providing a microclimatic analysis of different courtyards in Vienna. The goal of this research is to analyze the thermal behavior of different courtyards and compare them to adjacent street canyons in terms of temperature, humidity, wind speed and CO_2. Data was simultaneously recorded by mobile weather stations.

TABLE OF CONTENTS

Abbreviations

UHI Urban Heat Island

UHII Urban Heat Island Intensity

SVF Sky View Factor

H/W Height to Width Ratio

CO_2 Carbon Dioxide

BWF Built Walls Fraction

PSF Pervious Surface Fraction

Acknowledgements

I would like to thank my supervisor Prof. Mahdavi, who has guided and helped me through the process of writing this thesis. I would also like to thank Milena Vuckovic as well as the entire Department of Building Physics and Building Ecology at the Vienna University of Technology for their support in realizing this project and for providing me with the necessary equipment to perform my measurements. Furthermore I would like to thank Jasmin, Pilar, Daphne, Marcelo and Clyde who have spared the time to come with me and perform measurements around Vienna.

I would also like to thank my family who has morally encouraged and financially supported me during these last years and made it possible for me to concentrate on my studies.

1. INTRODUCTION

1.1 Objective

The objective of this research is to analyze the microclimate of geometrically different types of courtyards located in the inner districts of Vienna, Austria and compare it to the microclimate of adjacent street canyons. Through simultaneous measurements, this work aims to identify similarities as well as differences between the two and possibly explain significant differences. The overall objective is to contribute to the research in the field of urban heat islands and thermal comfort in cities.

1.2 Structure

This paper starts with an introduction in chapter 1 explaining the motivation preceding and leading to the execution of this research. The introduction also offers background information on the urban heat island phenomenon and on the emergence and use of courtyards. Some information is also given on important geometric and thermal properties of courtyards. Furthermore a concise overview of work published by leading researchers in the field is presented.

Chapter 2 contains the methodology of this research by describing each of the chosen measurement locations as well as the different types of measurements, which were performed.

In Chapter 3, the most important results of the measurements performed are presented in form of different types of graphs, including information on temperature, absolute humidity, wind and CO_2.

The main discussion and findings are then presented in Chapter 4, followed by a short conclusion and ideas for future research.

1.3 Motivation

An extensive array of previous and ongoing research has acknowledged the Urban Heat Island phenomenon (UHI) as one of the most challenging phenomena that urban life is facing today (see for example, Gartland 2008, Kleerekoper et al. 2012, Laaidi et al. 2012, Stewart and Oke 2012). Future urbanization projections suggest that urbanization worldwide will reach around 80% of an estimated global population of 10 billion by the year of 2050. Hence, an increasing number of people will be affected by the negative impacts related to the UHI effect (WBCSD 2010). Furthermore, the very phenomenon of urbanization is expected to lead to an intensification of UHIs by creating denser and larger urban areas. Negative implications of UHIs may lead to an increased electricity demand for cooling and consequently to an increase in greenhouse gas emissions, as well as to negative implications for human health and comfort (Gartland 2008).

As noted by Laaidi et al. (2012), during excessive heat events such as was recorded in France in 2003, heat related mortality can increase significantly. During that summer in 2003, baseline values where surpassed by a tripling, amounting to a total of 15000 heat related deaths in France alone.

Energy Demand

Urban heat island intensity (UHII) is defined as the difference between the temperatures simultaneously recorded in a city and in a nearby rural area. The UHII recorded at different locations varies depending on the local climate as well as the geometry of the city but in extreme cases can go up to 10 K in hot climates. Such a dramatic temperature increase inevitably will lead to a higher energy demand for cooling, which in turn leads to an increase of pollution in form of greenhouse gas emissions and to a reduced efficiency of air conditioning systems (Karlessi et al. 2009).

The data in Figure 1 is based on energy data compiled in the World Energy Outlook Reference Scenario and shows that the final energy consumption of buildings accounts for roughly 40% of total primary energy demand surpassing the energy consumption of both the transport sector as well as Industry and Manufacturing. Buildings furthermore account for one third of total greenhouse

gas emissions. This however should not only represent an enormous potential increase in cooling demand for buildings leading to a significant increase in energy consumption, and therefore emissions, but also a real potential for future energy efficiency and saving plans.

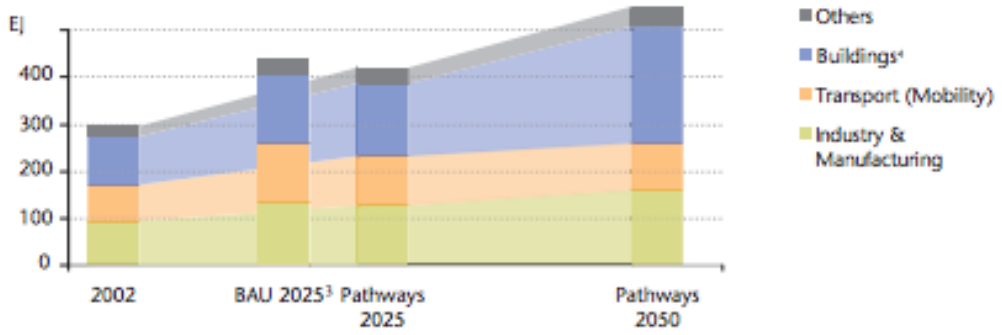

Figure 1: Levers for changing energy intensity: final energy consumption by sectors (source: WBCSD 2010)

Human Thermal Comfort

When human living and working areas are primarily located within the centrally positioned urban domains, that might face severe overheating circumstances during summer season, we can expect to have a negative effect on human health and thermal comfort. The exposure to thermal stress can impact human health and productivity and also decrease overall tolerance to other environmental stress factors (Epstein et al. 2006).

Human thermal comfort is however not only dependent on air temperature but rather on the combined effect of air temperature as well as air humidity, solar radiation and wind speed. For example, this cumulative effect may be expressed by the Physiologically Equivalent Temperature (PET), which is a complex measure based on the energy balance of the human body. Compared to other bioclimatic indexes, the PET index is of advantage because it uses the widely known unit °C. Furthermore the PET is a universal index for indication of bioclimate which can either be displayed graphically as temporal distribution or as spatial distribution in form of bioclimate maps (Matzarakis et al. 1999). The PET index was recently used in a study on spatial variability of urban heat islands and

thermal comfort in Rotterdam (Hove et al. 2015). Results have shown that on a microclimatic scale, shade by trees, altering wind patterns as well as radiation from surrounding buildings may have strong effects on the PET even on a small spatial scale.

The human body absorbs heat from direct and indirect radiation as well as from objects warmer than body temperature and conduction from air at above skin temperature. Heat can be released by exhalation, transpiration and radiation to the air as well as cold surfaces. Although the human metabolic system has numerous adjustment systems to deal with heat imbalances, extreme conditions can afflict serious damage to these systems as well as to general human health. Common risks include cardiovascular illnesses such as syncope, the failure to maintain blood pressure and oxygen supply to the brain. More severe consequences include organ failure due to heat stroke, which may lead to death (Conti et al. 2005).

Indirectly, higher temperatures offer favorable conditions for the formation of ground-level ozone through photolysis, resulting in decreased lung function as cardio-respiratory inflammatory diseases (Kleerekoper et al. 2012). While rural surfaces cool off more effectively through evapotranspiration soon after sunset, urban fabric is characterized by higher heat capacity and lead to warm surfaces past evening hours, when the human body is supposed to regenerate from heat (Shahmohamadi et al. 2011).

People who bear the highest risk of being affected by extreme heat conditions include small children, the elderly as well as people with medical conditions. It is thus of utmost importance to understand the reasons for such extreme temperature conditions and to find mitigation measures which can alleviate its negative effects such as increased mortality and morbidity rates (Conti et al. 2005).

2. BACKGROUND

2.1 The urban atmosphere

Earth's atmosphere consists of 4 different layers. For this work, the lowest layer is of importance, namely the troposphere, which is influenced by the earth's surface as well as by human activity. The troposphere consists of two different layers, the planetary boundary layer (PBL) or the mixing layer and the free troposphere. The mixing layer is, depending on the sun irradiation and the time of the day about 2 kilometers high. During the day the earth's surface is heated up by the suns' short wave radiation, which in turn heats up the air right above the ground. When the air warms up and expands, thus becoming lighter and starting to rise, it may form an inversion, which is a condition that most significantly favors the formation of urban heat islands. Such inversions may also trap warm air and pollution close to the ground (Gartland 2008).

Urban areas tend to have a higher heating rate of ground surfaces compared to rural areas, thus producing thicker and warmer boundary layers. As seen in Figure 2, the urban atmosphere is more complex, because it does not only have the surface and mixing layer such as the rural boundary layer, but consists of 3 layers including the urban canopy layer which reaches from the ground to the average height of roofs, the urban roughness layer and only then the mixing layer (Voogt 2004).

According to Oke (1978), the microclimatic significance of these different layers lies in the complexity of airflows and other three-dimensional effects caused by roughness elements. Specific effects are strongly dependent on the characteristics of these elements, such as shape, material and density.

While the effects of urban heat islands can be considered as beneficial in colder cities, where this excessive warmth may reduce heating demand, the negative effects in hot climates and during summer are prevalent (Gartland 2008).

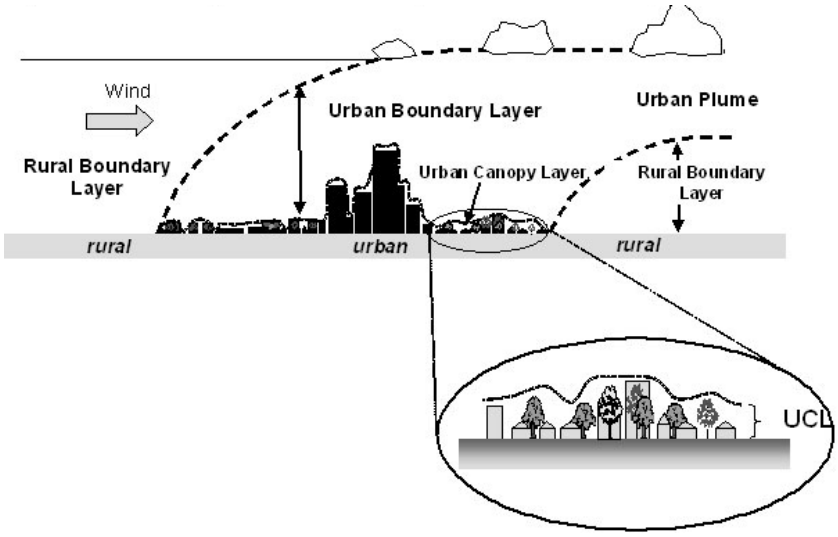

Figure 2: Main components of urban atmosphere (source: Voogt 2004)

2.2 Microclimate

While considerable temperature differences between urban and rural environment have been extensively documented, urban heat islands do not merely represent one big island above a city, but rather make up a cluster of several small islands, which can be the result of different physical processes (Krätschmer 2010, Mahdavi et al. 2014, Dimitrova 2013).

These small-scale variations belong to the realm of urban climates, or microclimate. A microclimate refers to the distinctive climatic features of relatively small areas, such as a garden, a park or a courtyard. It can be identified and measured by temperature (usually expressed in Kelvin), rainfall, humidity and wind speeds and will usually differ from the overall climatic conditions of the entire area above (Met Office 2011).

Microclimates can strongly be influenced by either the morphology or geometry of the concerned area as well as by the physical properties of its surfaces (Dessi 2011). Dessi (2011) studied thermal capacity, albedo and the density of materials, arguing that it affects the unpleasant microclimate in cities, especially during summertime. More specifically, spaces enclosed by walls and covered by different types of stone and stone mixtures lead to significant surface temperature increases depending on the efficiency of the walls in obstructing airflow and the specific heat capacity of the materials. It is thus vital to recognize how different

urban structures facing specific climatic circumstances can significantly alter microclimatic conditions. A city therefore will harbor a cluster of many different microclimatic conditions, making the study of urban climate a complex matter.
In this context, it can be said that studying urban microclimate is strongly linked to the study of urban heat islands. Therefore, this research aims to provide a comprehensive analysis on a microclimatic scale, more precisely documenting the differences between geometrically different courtyards and adjacent street canyons.
As it can be seen in the spatial map of Vienna's inner districts (Figure 3), densely built urban fabric is revealing significant amount of courtyards that may be thermally affected by the surrounding buildings.

2.3 Why courtyards?

As can be seen in Figure 3, the general urban fabric of Vienna, and most European cities, is composed of buildings with courtyards. The large amount of courtyards can be expected to play their role in the occurrence and intensity of the UHI phenomenon and therefore could be key in formulating proper mitigation measures.

Figure 3: Map of Vienna's city center (source: Google Maps)

A courtyard in its traditional layout can be defined as an enclosure by buildings or walls on two or more sides, which is open to the sky. The courtyard as an architectural tool stems from hot and arid regions. The traditional uses, as one of the oldest architectural footprints of humanity, are primarily social in nature, including family as well as community activities ranging from gardening, cooking over to sleeping. The thermal conditions inside the courtyard are directly linked to the amount of incoming solar radiation, indicating that the orientation as well as the height of the surrounding walls could have a significant effect (Almhafdy et al. 2013).

While courtyard design immediately affects the effectiveness of its uses as well as its specific functions, utility has not been the only source of modern change in variation of courtyard configurations. Designer creativity is among the reasons for the creation of innovative designs including modern shapes with sometimes semi-enclosure of two or three walls, which may also improve microclimatic conditions (Almhafdy et al. 2013).

As described by Tsianaka (2006), courtyards have become a central part to Athens' urban morphology due to high building density and serve as a ventilation means for back rooms. In her research she tried to quantify the influence of urban geometry on the climate of Athens and used two different areas of the city. Outdoor temperatures as well as indoor temperatures were recorded in rooms looking to either the street or the courtyard. In both areas, the rooms facing the courtyard demonstrated significantly lower temperatures than their street counterparts, with a maximum difference of 5.1 K. More specifically, this research has shown that in areas of high building density narrow courtyards are more beneficial than wider ones (Tsianaka 2006).

The general assumption of improved thermal comfort within courtyards should however be carefully checked through the specific microclimatic conditions at any given location, which will depend on the type of courtyard, its orientation, geometry as well as physical properties of building materials (Meir 1995).

2.4 Urban Heat Islands

Urban heat islands are identified in cities worldwide, representing a "reverse oasis" with higher air temperatures occurring in cities when compared to their rural surroundings (Gartland 2008). First discoveries of urban heat islands date back to the beginning of the 19th century, where artificial heat excesses have been identified in London, Paris and Vienna (Gartland 2008).

It can be said that the design and climate of a city have a relationship, which is marked by reciprocity. On one side, the local climate affects the orientation, design and specific characteristics of a city. On the other side the very collection of buildings, urban canyons and morphology influence the surrounding climate through their thermal characteristics and morphology.

Such relationship is manifested in varying air temperature, solar irradiation, precipitation, wind and cloud cover. These variations are not uniform over the urban area, but display strong variations within several meters.

Hence the urban heat island effect results not only in the air temperature differences between the city and its rural surroundings but also displays considerable variance across a city due to meteorological and urban characteristics Kleerekoper et al. (2012) lists seven causes for the urban heat island effect:

1. Solar short wave radiation is absorbed by common construction materials such as concrete with low albedo and hence low back scattering, resulting in heat storage also caused by multiple reflections between building and street surfaces.
2. Long wave radiation emitted by the earths' surface is absorbed and reemitted into the urban environment by local air pollution such as particulate matter.
3. The height of buildings leads to obstruction of the sky and hence causes for long wave radiation to be trapped inside the urban canyon again by principles of absorption and backscattering.
4. Anthropogenic release of heat due to combustion processes, mainly attributed to traffic, district heating and industry.

5. Increased heat absorption capacity of urban building materials as well as the increased surface of a city compared to a rural area.
6. Less vegetation and increased use of impermeable materials leads to a reduction in evaporation compared to rural areas, resulting in an increased energy input into sensible heat as opposed to latent heat, therefore leading to stronger temperature fluctuations.
7. Cities cause reduced wind speeds, therefore also reducing turbulent heat transport within streets.

The UHI effect is strongest during calm and warm days, because of increased sun irradiation and slower dispersion of heat due to lower wind speeds (Kleerekoper et al. 2012).

As was explained in the previous section, the UHI effect brings numerous severe negative effects to both urban areas and city dwellers. However, carefully planned mitigation measures are expected to bring significant improvements to the urban communities.

2.5 Urban morphology

This sub-chapter aims at explaining in more detail the most influential factors on the microclimate of courtyards.

According to Oke (1987) the urban climate and hence the formation of UHI is most strongly influenced by urban morphology. The total amount of urban surface is increased compared to an unbuilt planar surface. This means that more surface is available to interact physically as well as thermally with the surroundings. The geometry of these urban structures may provide shade, alter wind speeds, retain and reradiate heat. Depending on the materials predominantly used for urban structures, their absorption, retention and emission of radiation can vary strongly. As put forward by Stewart and Oke (2012), most research on UHI relied on the differentiation between “urban” and “rural”, which can be problematic since these terms have no single, objective meaning and are hence irrelevant for climatology. Consequently, they combined some of the features of previous terrain classifications made by other scientists to come up with a division of urban terrain

into 7 urban climate zones (UCZ). Most importantly these zones are characterized by urban structure, building material and permeability. While structure influences the airflow and atmospheric heat transport, building materials influence their surroundings by their albedo and hence heating/cooling potential as well as moisture availability.

An important indicator for urban geometries is the sky view factor (SVF). It expresses radiative properties, namely the ratio between the received radiation on a flat surface and the entire hemispheric radiating environment. More specifically, this means that if seen from any point of that planar surface, the totality of the hemisphere is visible and hence no obstruction occurs, the SVF value is 1. This implies the maximum possible exposure to incoming solar radiation. The value of the SVF will decrease with increasing obstruction of the sky seen from the initial surface and will reach 0 when the totality of the sky is obstructed and hence no solar radiation can reach the ground (Vieira and Vasconcelos 2003).

2.5.1 Street Canyons

For the purpose of this research, street canyons are used as a medium of comparison to courtyards. Street canyons make up a large part of any city and are subject to most human activity such as transportation or leisure. Street canyons, referring to streets that are enclosed by buildings on both sides, are found to often have compromised thermal human comfort conditions due to several reasons (Meir 1995). Beyond street orientation, similar influencing factors as for courtyards have been investigated. While street orientation seems to have the strongest effect on local thermal conditions, height to width ratio as well as surface morphology play a significant role (Dimitrova 2011). Furthermore, a study on the climatic impact of vegetation was performed in 9 climatically different cities (Alexandri and Jones 2008). This study revealed that green walls and roofs had a cooling effect on the canyon air.

2.5.2 Surfaces

The intensity of urban heat islands can vary strongly depending on the materials that are used to cover urban space. This is due to the ways in which the materials react with incoming solar radiation and precipitation. The initial amount of incoming sun radiation plays a critical role in determining climate generally. The UHI intensity then depends on the physical properties of surface materials such as albedo, porosity and permeability, which directly influence the surrounding microclimate. The choice of material can influence the range of peak surface temperature by several tens of degrees (Dessi 2011).

The following section will explain the most prominent surfaces, which can be found in courtyards as well as in street canyons. A good number of studies have looked into innovative ways to overcome these typical properties in order to improve thermal conditions by achieving considerable temperature reductions, energy savings and consequently human comfort, air quality and storm water runoff (see for example Gartland 2008, Scholz and Grabowiecki 2007).

Cool paving and vegetation cover are among the most beneficial and most applicable techniques in courtyards, identified by Gartland (2008).

2.5.3 Green surfaces

Vegetated surfaces, as opposed to sealed surfaces, have a different mass and energy balance. According to Oke (1978), this directly relates to latent (no temperature change) and sensible heat fluxes (temperature change) as well as the physical heat storage system and the biochemical energy storage system of plants. Air temperature and humidity are only indirect parameters referring to the water and radiation balance in the atmosphere. Hence, the differential heat and energy storage systems of plants are expected to have a direct impact on air temperature and humidity. Physical heat storage refers to the absorption and release of heat by all parts of the plants, including leaves and stems. Biochemical energy storage refers to the chemical process of photosynthesis.

The energy balance of vegetated surfaces can be summarized as (Oke 1978):

$$Q = Qh + Qe + \Delta Qs + \Delta Qp \qquad (1)$$

where Qh is latent heat Qe is sensible heat, ΔQ_S refers to the net rate of physical heat storage and ΔQ_P represents the net rate of biochemical energy storage due to photosynthesis.

Plant leaves show radiation emissivity and reflectivity behavior depending on the wavelength of incoming radiation. While blue and red light of the visible electromagnetic spectrum are useful for photosynthesis, these wavelengths are strongly absorbed by leaves. On the other hand, near infrared light and other energy intensive wavelengths, which are not useful for the chemical process of photosynthesis are reflected to protect leaves from overheating and result in energy intensive radiation being reflected back into the atmosphere. At the same time, leaves are strong absorbers of long wave radiation and hence it can be assumed that vegetation absorbs incident long wave radiation from for example built surfaces before it reaches impervious ground surfaces (Oke 1978).

Trees and vegetation are an important component to urban life. The positive effects of plants as surface coverage range from passive temperature reduction through shading to active processes of air quality improvement through photosynthesis. Trees and other plants use the heat by surrounding air in order to evaporate the water, which they have previously absorbed through their roots (Gartland, 2008). Vegetation is used on floor surfaces as well as roofs and even facades in modern architecture. This does not merely improve the temperature and air quality conditions of buildings but also has positive esthetic effects on the urban landscape. Green areas are known to improve the wellbeing of humans. Experiments have shown that the cooling effect by tree leaves reduces temperature on the surface underneath by up to 20 K (Meier 1990).

Within courtyards vegetation and trees can play a significant role in increasing evapotranspiration and therefore reduce ambient air temperatures. Furthermore strategic positioning of trees for shading purposes can significantly reduce energy demand for cooling. A joint study by the Lawrence Berkeley National Laboratory and the Sacramento Municipal Utility District has shown that the energy demand

of buildings can be reduced by up to 40% when trees were oriented to west and southwest of the buildings (Gartland 2008). Numerous different types of trees, bush and other vegetation are applicable for greening courtyards. When making a choice, one should be aware that evergreen and deciduous plants both have their own but different advantages during wintertime. While the former provides shielding from incoming wind, the latter allows for the little available solar radiation to improve thermal comfort (Gartland 2008).

2.5.4 Paved surfaces

Paved surfaces make up almost half of all urban surfaces and have become a dominant feature of the urban landscape. The majority of paved surfaces being made of either asphalt or concrete have strong influences on urban heat islands and therefore on human comfort due to their thermal characteristics. The specific performance of pavement depends on indicators of the used material such as permeability, thermal conductivity, emissivity and porosity (Dimitrova 2013).

Asphalt is initially very dark, having a solar reflectance of only 5%, which over time can increase to roughly 20%. During summertime it can heat up to 65°C, making it the second hottest feature of the urban landscape after conventional roofing materials. Concrete on the other hand starts with a light grey and slightly higher solar reflectance of 30-40%, which decreases as concrete becomes darker by dirt over time. Concrete can heat up to a maximum of 50°C (Gartland 2008). These specific thermal properties of both materials as well as the albedo can be seen on the thermal images of Figure 4.

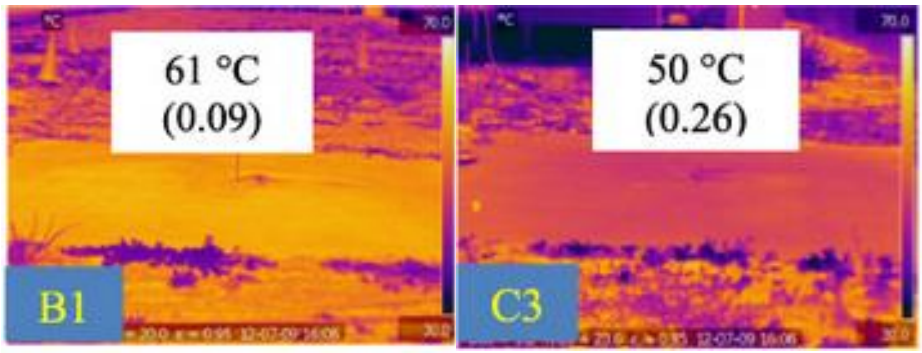

Figure 4: Optical and thermal images of experimental test sections: B1 is asphalt and C3 is concrete (lighter is hotter, average surface temperatures are listed with albedo in parentheses) (Source: Li et al. 2013)

Both materials absorb and retain solar radiation. This is due to a greater heat capacity and thermal inertia compared to rural soil and vegetation. The greater retention of heat results in the materials cooling off less effectively and re-emitting a great amount of heat during nighttime, therefore keeping temperatures high when there is no incoming solar radiation (Shahmohamadi et al. 2011).

Researchers have come up with a number of possible mitigation measures. For example, the addition of white pigments to the concrete surfaces in order to increase albedo were studied by Akbari et al. (2001) and results show that surface temperatures can be reduced by up to 10 K. Newer technologies allow for the production of pervious concrete, a possible solution for most problems related to regular concrete. Pervious concrete allows rainwater to reach the ground underneath, contributing to recharging groundwater and reducing storm water runoff (Tennis et al. 2004).

Permeable pavements have a higher amount of air voids compared to their impermeable counterparts. Such design allows for water to seep through the pavement and reach the sub-layers and all the way down to groundwater reservoirs. Permeable pavements are applicable for most urban surfaces with the exception of high-speed traffic areas. The benefits of such pavements are numerous. For wastewater management, permeable pavements allow for a reduction in storm water runoff, which can be problematic depending on the urban water systems. For the urban climate, such pavements offer improved outdoor

thermal conditions through higher amounts of water being available for evaporative cooling which consequently does not only cool the surface but also the ambient air (Li et al. 2013).

Scholz and Grabowiecki (2007) developed this idea further in their research. The pervious pavement does not only collect storm water to then recharge groundwater. They furthermore suggest the installment of a sub-base system, which would allow for buildings to utilize the heated water and hence save energy. Another disadvantageous characteristic of typical pavement materials is the lack of ability to store water inside the material, which later can evaporate through solar radiation. This ability is also called porosity and its absence leads to lower than normal evaporation rates in the city, negatively affecting local air quality. A model simulation by Nakayama et al. (2010) could show that increased pavement porosity could decrease the above air temperature by 1-2 K more than above a green surface, therefore improving thermal comfort. The only disadvantage of such innovative systems is the risk of clogging.

Such innovative pavement technologies are also known as cool pavements include permeable pavements, high-reflectance pavements, evaporative cooling pavements and shade-cooled pavements. They are named as such because they can reduce their own surface temperature as well as that of the near-surface air and hence provide mitigation potential for urban heat islands (Li et al. 2013).
As seen in the last section, there are two different ways to make paved urban surfaces cooler. Firstly, we either increase their solar reflectance or albedo. Secondly, we can make them more permeable and hence allow for more water to seep through the material and then evaporate when solar radiation is high.

Several experiments, which have modeled the effects of light pigmentation and increased permeability of considerable surface fractions in larger American cities, have shown that important microclimatic improvements can be achieved (Gartland 2008). It will thus be important to consider such measures as possible options in mitigating the UHI effect in cities all over the world.

2.5.5 Albedo

The albedo of surfaces is a useful parameter in order to compute the energy balance. It describes the ratio of incoming light that is backscattered into space by an object and its value lies between 0 (object that appear black to the human eye or backscatter very little light) and 1 (objects that appear very bright and backscatter a large fraction of incident radiation) (Hanner et al. 1981). Cities usually have a smaller albedo than their rural surroundings. Surfaces with a lower albedo absorb a higher fraction of incoming radiation and hence heat up more. We can thus expect surfaces with lower albedo such as are prominent in the urban fabric to retain considerably more heat and hence deduce that albedo plays an important role in UHI intensity (Taha et al. 1988).

Taha et al. (1992) studied the specific temperature differences of surfaces with different albedos. They concluded that surfaces with low albedos of 0.1 may heat up to 30 K more than the surrounding air temperature, while high albedos of 0.6 and above reduce the temperature difference between material and air to about 5 K. Figure 5 shows the systematic decrease of surface temperatures with increasing albedo.

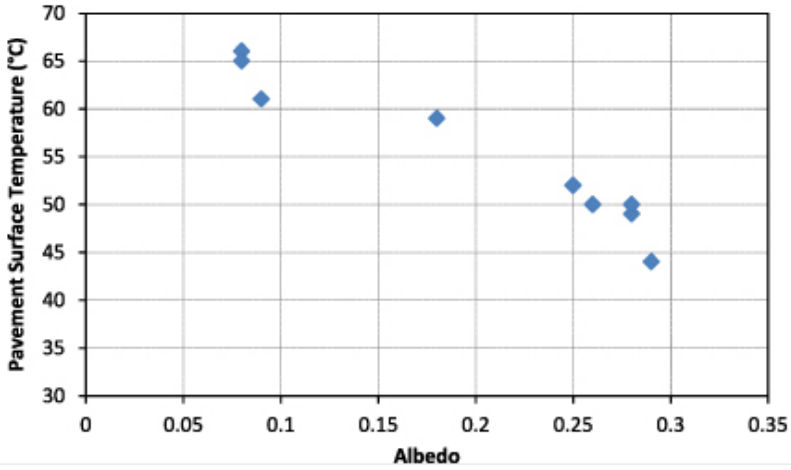

Figure 5: Effect of albedo on pavement surface temperature (Source: Li et al. 2013)

2.6 Literature review

The first part of this literature review will discuss the work previously done by the Department of Building Physics and Building Ecology (BPI) at the Vienna University of Technology. The second part will provide a review of existing literature in the field of urban climate, with focus on courtyards and their thermal characteristics, as well as outlining the general research on urban heat islands.

2.6.1 BPI Publications

Mahdavi et al. (2014) performed a major study on urban heat islands in 8 Central European cities. Results have shown that the UHI intensity is strongest during night hours. The study also established an important systematic framework including geometric and semantic variables. These were tested in their effects on UHI effects and urban microclimate variance.

Krätschmer (2010) deployed mobile weather stations, mounted on an adequate height of 1.6 meters, for a comprehensive analysis of urban canopy climatic conditions. The goal of this research was to describe the implications of the urban heat island effect on architecture and urban planning and to propose measures for mitigation. Results showed large differences within small areas, which are not sufficiently represented by single weather stations. These large differences could mostly be explained by looking at solar radiation and sky view, pointing to the influence of shading and urban geometry.

Hammerberg and Mahdavi (2014) concentrated the research on the specific role of trees in the urban energy balance, more specifically on the radiation exchange of the urban environment in Vienna. The relationship between the sky view factor and urban heat island intensity was examined, revealing that the SVF needs to be subdivided into measurements with and without tree information, since data shows a significant overestimation of the SVF when placed above the tree canopy. They noted that the influence is highest during night time, when long wave

radiation is kept within the urban canopy layer, so that the urban environment cools off much slower than its rural counterpart.

Dimitrova (2013) looks into possible UHI mitigation measures by documenting and characterizing the causes of the UHI effect in Vienna. By analyzing the long-term weather data she revealed distinct microclimatic patterns with respect to spatial, seasonal and hourly scale. Furthermore, she documented significant UHI intensity with distinct nocturnal features. Measurements are taken in two different street canyons, one with trees and the other without trees. Surface characteristics together with the obtained meteorological data lead to the conclusion that the possible UHI mitigation suggestions may be the overall increase in the albedo of pavements – such as changing from black asphalt to concrete, as well as the increase of albedo for surrounding building surfaces. Furthermore, Dimitrova noted that trees certainly help mitigate extreme summer conditions.

2.6.2 International Publications

In the field of urban heat islands, an extensive array of research has been performed on an international level. In her book "Urban Heat islands", Gartland (2008) explained the causes and typical characteristics of the urban heat island phenomenon. She furthermore introduced important mitigation measures such as cool paving, cool roofing and the use of vegetation, pointing out the importance of raising awareness and acting on a phenomenon, whose negative effects are yet to be widely known.

Oke (1987) has consolidated an enormous amount of important information in his book "Boundary layer climates" for understanding all the physical and chemical processes which contribute to the formation of urban heat islands. He furthermore published an important paper in 2012 together with Stewart, recognizing the problem of defining an area as "urban" or "rural" and therefore classifying areas into 17 different "Local Climate Zones" (LCZ) (Stewart and Oke 2012).

Myrup (1969) created a numerical model based on an energy budget to quantify and qualify the urban heat island effect. Several physical processes are attributed to the net effect of urban temperature excess. While some of them manage to cancel each other out within the urban environment, the decreased evaporation at the city center, reduced wind speed and the properties of paving materials seem to play the most crucial role in creating a temperature contrast between urban and rural area. While evaporation plays a larger role during the daytime hours, thermal properties of surfaces are most important at night.

Several studies have been published on the use of courtyards, their microclimatic conditions and their role in the urban heat island effect. Courtyards have been investigated for their thermal characteristics and their role in offering improved human comfort especially in hot and dry regions by a number of scientists.

Lobo (2015) investigated the importance of the traditional use of courtyards as a medium for improving human comfort. Alongside the general use of buildings to shade streets and courtyards, she further points to the difference in courtyard uses between developed and developing countries. In the former the impact of an increasing trend for mechanical air conditioning and a lower tolerance limit to harsh climate conditions alongside higher incomes have significant effects on how courtyards are being used.

Ali-Toudert and Mayer (2005) have performed some research in the area of thermal human comfort and its dependence on street design in hot and dry regions. Most decisive factors included the street orientation and H/W ratio. The investigation offered thorough spatial and temporal analysis by the aid of a three-dimensional model ENVI-met, designed to simulate microclimatic models of short wave and long wave radiation fluxes between buildings and their environment. Results have shown that shading is the most crucial strategy in order to improve human thermal comfort, achievable by either vegetation or building design.

Meir (1995) performed microclimatic measurements at two different semi-enclosed courtyards in the Negev Desert, Israel. His result showed clearly, that first of all, even semi-enclosed spaces generate their own microclimatic conditions. The detected variances between courtyards were attributed to geometry. The extent of direct solar exposure due to orientation and the importance of ventilation for the exhaust of hot air are the most important explanatory factors in his research.

Almafdy et al. (2013) performed another study on the microclimatic performance of courtyards. Previously acknowledged as micro-climatically determining design variants, such as H/W ratio and orientation were investigated through an institutional scale U-shaped courtyard in Malaysia. This study combined simulation with experimental measurements of air temperature, humidity and wind patterns. Results showed that primarily the height of the walls enclosing a courtyard influences the inside air temperature.

3. METHODOLOGY

3.1 Measurements

This thesis aims to analyze the microclimatic circumstances of different courtyards in the inner districts of Vienna and then compare them to the microclimate of the adjacent streets. In order to do so, a series of measurements have been performed.

Usually, fixed weather stations are positioned at altitudes above the average building height, or are installed on building roofs. In order to acquire the data that is required for the abovementioned analysis (such as small scale variations), the use of mobile weather stations is necessary. The mobile weather stations (as seen on Figure 6) used are mounted on bicycles and hence measure at a height corresponding to the average height of a human being (160 cm); furthermore they can be taken directly into the courtyards and the street canyons chosen for data acquisition.

Figure 6: Mobile Weather Station

The data acquisition was subdivided into two different phases. In the first phase, 10 different locations in Vienna, Austria were chosen (See Table 1 in Location Profiles). Each location consisted of 2 measurement points; one within the

courtyard and one positioned at the adjacent street (located right outside the chosen courtyard). Measurements were conducted using two mobile weather stations, which were attached to bicycles. Each measurement unit monitored the microclimatic circumstances for four consecutive hours (13:00-17:00) simultaneously. Each location was measured on a different day between April and July 2015.

For this first phase of data acquisition, further technically similar measurements were conducted at 3 of the 10 locations (Paniglgasse (P1), Richtergasse (R1) and Miesbachgasse 15 (M3)) during morning and night hours (See Table 1 in Location Profiles Section). Since air temperatures within an urban canyon are dependent on the incoming short wave radiation, as well as on the long wave back radiation from the urban surfaces, it can be expected that the overall urban overheating is prolonged in its duration by the long wave back radiation, and especially pronounced during hours after sunset (Hammerberg 2012). Hence a series of nighttime measurements were undertaken at the 3 locations between 20:00 and 24:00. For this measurement series, the weather stations were positioned in the same way as for the afternoon measurements, recording data simultaneously in the courtyard and on the street. Each location was measured on a different day between June and July 2015.

In the same way as for the night measurements, a series of morning measurements have been performed at the same 3 locations. Data was recorded between 08:00 and 12:00. This set of data may reveal important information on whether urban overheating is carried differently into the morning hours in courtyards than on streets. Secondly, morning measurements can show if there are differences in heating rate of the air at courtyard and street level.

This first phase serves to compare the microclimate of courtyards with the microclimate of streets. Data between courtyards however cannot be directly compared, since measurements at each location were taken on different days. Furthermore, the data sets of the first phase are limited to 4 consecutive hours, since the bicycles could not be left unattended at the street. Measurements were

taken with an interval of 5 minutes for all data sets. The resolution of the data for the first phase was then reduced averaging the original data recorded.

A second phase of data acquisition was therefore performed in an additional 4 courtyards, which are also located within central Vienna (See Figure 10). Temperature and humidity sensors were fixed at each location by attaching it to the railing of a balcony, facing the courtyard. The data acquisition took place simultaneously at all 4 courtyards for a consecutive period of 3 weeks between July 8th and July 29th. The data recorded during this phase may offer insight on the thermal behavior of courtyards over 24-hours periods under different weather conditions. Furthermore data from the second phase allows comparing different types of courtyards, since the data was recorded simultaneously.

3.2 Equipment

All the measurement equipment sensors and data loggers are mounted on two different bicycles. As can be seen on Figure 6 the equipment is attached to the rear of the bicycle and can thus be transported with ease to the numerous different measurement locations.

The first bicycle is equipped with a temperature and humidity sensor, a low power anemometer for wind speed (Vector Instruments Type A100L2) and a pyranometer for solar radiation (Skye Instruments), all connected to the same logger (Weatherstation DK-Stat1, Driesen + Kern GmbH). The second bicycle is a three-wheel e-bike, which is also equipped with the same temperature, humidity sensor, a pyranometer and a low power anemometer for wind speed, all connected to the same logger. Additionally, both bikes were equipped with Telaire 7001 CO2 / temperature monitors connected to two Synotech onset HOBO data loggers. Launching and reading of the weather stations is done using the HOBOware Software. The measuring and recording intervals were set to 5 minutes. The loggers for the CO2 measurement were also set to a 5-minute interval. The data can then directly be downloaded onto a personal computer using the HOBO software (HOBOware 2015).

For the second phase of data acquisition, the same type of temperature and humidity sensors were directly fixed onto the balcony railings as can be seen on Figure 7. To determine the Sky View Factor, pictures at each courtyard were taken using a fish eye camera lens. The digital picture was then translated into a SVF value using a tool called Sky View Factor Calculator, which was developed by the University of Gothenburg, Sweden, using Mathworks Matlab and Matlab Compiler Runtime (MCR) (University of Gothenburg 2015).

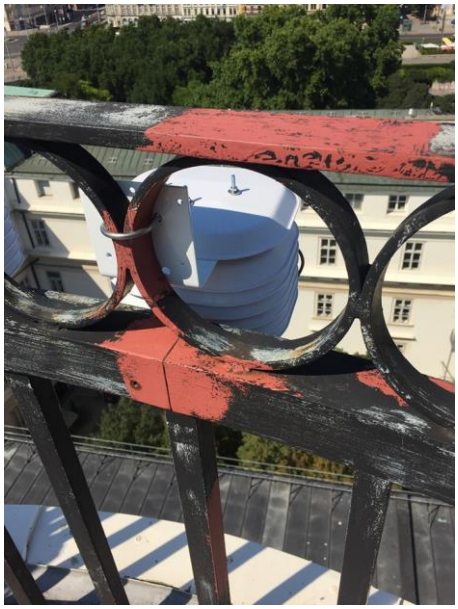

Figure 7: Temperature and humidity sensor fixed on balcony railing

3.3 Parameters

The parameters explained below include those climatological parameters, which were measured by the mobile weather stations as well as some geometrical parameters, which were measured with online mapping tools.

Classical climatology of the first of half of the 20th century almost exclusively deals with the central climatological parameters such as ambient air temperature and humidity, which are also central to this study. It is however crucial to remember, that these are only indirect measures of more fundamental quantities (Oke 1978).

Air Temperature [°C]: This is the most important parameter in identifying the urban heat island phenomenon, since urban heat island intensity and occurrence is defined in difference between urban and rural temperatures [K]. UHI intensity is defined by the following formula (Oke 1987), where ΔT is the temperature difference, Tu is the urban temperature and Tr is the rural temperature.

$$\Delta T = Tu - Tr[\mathrm{K}] \quad (2)$$

Absolute Humidity [g/kg of dry air]: Absolute humidity *W* was calculated using the relative humidity values recorded by the humidity sensors. The same method and series of equations were used as in the work of Dimitrova (2011). The first step was to calculate the saturation vapour pressure *E* (Equation 3) to determine the vapor pressure *e* (Equation 4). The next step was then to calculate the partial pressure of dry air p_a (Equation 5) in order to then find the total pressure $P_{tot.}$ The results of these three formulas were then used to find the absolute humidity with Equation 6. The results were multiplied by 1000 to modify the results from kg/kg to g/kg dry air.

$$E = 611.2 * \exp(17.08085 * T / (234.175 + T)) \ [\mathrm{Pa}] \quad (3)$$

where *E* is the saturation vapour pressure and *T* - the temperature in °C.

$$e = \varphi * E / 100\,000 \ [\mathrm{kPa}] \quad (4)$$

where *e* is the vapour pressure, φ – the relative humidity, and *E* the saturation vapour pressure from the previous equation.

$$p_a = \rho_a * T / 0.0035 \ [\mathrm{kPa}] \quad (5)$$

where P_a is the partial pressure of dry air, ρ_a – the density of dry air and *T* - the air temperature in K.

$$P_{tot} = p_a + e \ [\mathrm{kPa}] \quad (6)$$

where P_{tot} is the total pressure, p_a is the partial pressure of dry air from equation 5 and e the vapor pressure from equation 4.

$$W = \epsilon * e / (P_{tot} - e) \text{ [g/kg dry air]} \quad (7)$$

Where W is the absolute humidity, ε is the ratio of molecular weight of water vapor to dry air (ϵ = 621.97), e is the vapor pressure from equation 4, and P_{tot} is the total pressure from equation 6.

Absolute humidity may be expected to be higher in courtyards with more vegetation and a higher ratio of permeable surfaces. Impermeable surfaces have less or no capacity to store humidity for prolonged evaporation and therefore the surrounding air is expected to be drier, which at very low levels can be associated with dry air problems such as skin and lung irritation. In terms of human comfort, temperatures are felt lower than they actually are at low relative humidity, while high relative humidity causes moisture to stay on surfaces and may cause severe discomfort. Similarly, a study performed by Tsutsumi et al. (2006) found out that the same moisture content level is perceived as drier in lower temperature conditions. Canadian meteorologists defined this interrelation between temperature and humidity as the "Humidex" (CCOHS 2015). The humidity index describes how hot the weather feels to the average person. Humans can be comfortable in a wide range of humidity levels, the ideal point however lies somewhere between 50% and 60% (Pearson 2007).

Carbon Dioxide [ppm]: CO_2 concentrations can vary considerably at a location over a period of time due to car traffic and other human related activities. CO_2 concentrations may also be influenced by vegetation. As shown in the measurements of Dimitrova (2011), when she compared a street without trees to a street with trees, CO_2 was actually higher in the vegetated street. Possible explanations for this are higher traffic intensity on the vegetated street but also the density of vegetation may actually deteriorate ventilation and retain pollutants within the urban canyon. As found by Gromke and Ruck (2007), the height as well as the size of tree crowns can have a direct effect on local air quality.

Concentrations furthermore may depend on dispersion through wind and hence wind direction in relation to street canyons.

Wind Speed [m/s]: Higher wind speeds lead to higher mixing of air within the planetary boundary layer, which in turn leads to a faster dispersion of heat emitted from urban surfaces. Wind speeds inside the courtyard and on the street will be measured and compared. Due to the complete enclosure of courtyards by walls, lower wind speeds can be expected within courtyards.

Pervious Surface Fraction (PSF): The fraction of surface covered by vegetation or simply the fraction of unsealed surface that covers the ground of a courtyard is denoted by a ratio called Pervious Surface Fraction (PSF). The following formula denotes this fraction, with values ranging between 0 and 1:

$$PSF = \frac{A(p)}{A\,(c)} \qquad (8)$$

Where $A(p)$ is the pervious area of the courtyard and $A(c)$ is the total area of the courtyard.

Built Walls fraction (BWF): The fraction of built surface (between 0 and 1) is the total area of building walls directly facing the courtyard and the ground surface in relation to the total area of the courtyard, which is defined as

$$BWF = \frac{A(w)}{A\,(c)} \qquad (9)$$

Where $A(w)$ is the area of building walls and $A(c)$ is the total area of the courtyard.

This fraction can give some information on the potential thermal long-wave back radiation by the building walls, provided the thermal properties of the wall surface materials are known. The larger the fraction, the larger the amount of wall area compared to the courtyard ground surface, the more radiation, once reemitted by

the building walls, might be trapped inside the courtyard. This can have a significant impact on the ability of the courtyard to cool down effectively over night.

Height to Width Ratio: This parameter is expressed as the ratio of the average building height surrounding the courtyards divided by the average width of the courtyard. This means that an aspect ratio above 1 refers to a case where the average height of the building walls surrounding each courtyard are greater than the average length of the courtyard itself. As was shown in a study by Ali-Toudert and Mayer (2006), the H/W ratio may have a decisive effect on human thermal comfort. In order to avert extreme heat stress, proper planning requires taking into consideration the H/W ratio combined with adequate orientation in relation to solar radiation. Effective design choices can be made, when street usage is known. As shown in figure 8, an increase of the H/W ratio may lead to lower air temperatures throughout a typical summer day. In combination with orientation, critical differences in air temperatures can be achieved, where an E-W orientation leads to higher temperatures and a N-S orientation shows slightly lower temperatures.

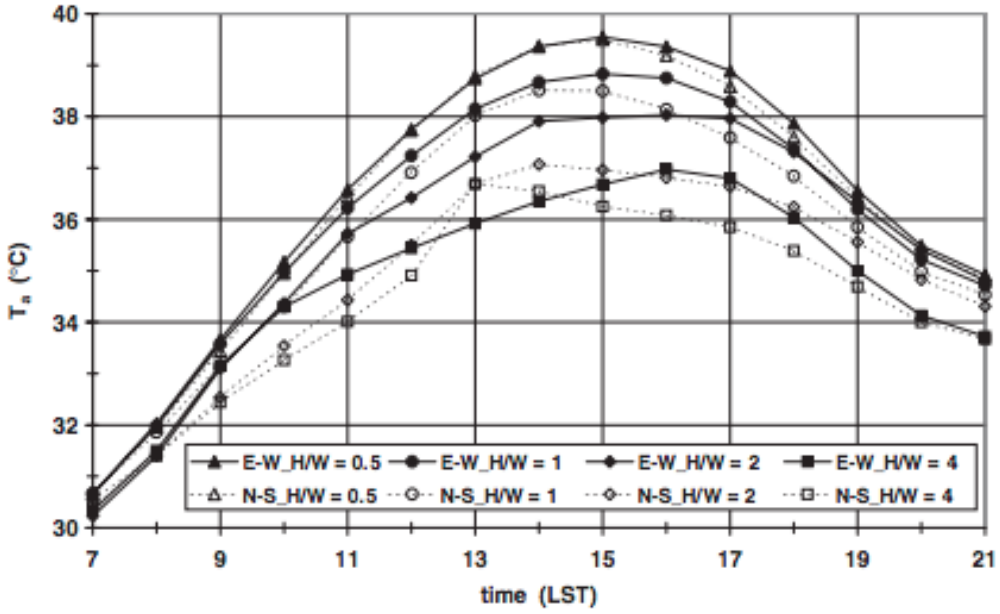

Figure 8: Diurnal variation of the simulated air temperature Ta at 1.2 m above the ground in the middle of the street canyons of an aspect ratio of H/W=0.5,1,2, and 4, oriented E-W and N-S, for a subtropical location on a typical summer day (Source: Ali-Toudert & Mayer 2006)

Sky View Factor (SVF): This parameter has previously been identified as the indicator that most strongly affects the intensity of urban heat islands. Being directly proportional to the amount of sun radiation that penetrates into the courtyard, this indicator can provide important information on the reasons behind the formation of the UHI and its intensity. The sky view factor is a fraction, which expresses the obstruction of the sky by buildings seen from a point on the earths' surface. This results in a reduced amount of sky being available for radiation exchange. The values range from 0 to 1, where 0 is the total obstruction of a surface point with no direct radiation flux to the sky, and 1 is an entirely unobstructed area. The SVF can be considered a primary contributor to the urban long wave radiation balance (Hammerberg 2014).

Research Questions

This paper will investigate microclimatic conditions within different types of courtyards and compare them to adjacent streets. Based on the findings from previous research, the following assertions will be tested in this work:

- If certain design conditions are met, courtyards generally display more favorable thermal conditions than the adjacent street.
- Courtyards create different microclimatic variances depending on their geometry.
- The H/W ratio of a courtyard influences its ability to effectively cool off over night.
- Courtyards represent a direct shelter from wind, reducing wind speeds compared to the street.
- CO_2 levels inside courtyards are expected to be lower than at street level.

3.4 Locations

The data for this study was collected at 14 different locations. All measurement locations are located within the inner nine municipal districts of the city of Vienna. This area, according to the principles of the urban heat island phenomenon, is expected to show the strongest intensity of the UHI effect compared to surrounding rural areas. This is partly due to the higher building density compared to suburban areas, as well as the prevalence of historic buildings, which usually means that there is a more extensive use of impervious building materials and relatively low amounts of green areas and vegetation, compared to newly built areas outside of the center.

For the first phase of data collection, 10 courtyards were chosen. The choice of courtyards includes a variation of different sizes, building heights, as well as types of green surfaces. As can be seen in Table 1, 5 locations do not have any green surfaces, while the other 5 locations have varying amounts and types of pervious surfaces and vegetation. Seven out of the 10 chosen locations are of small to medium size with less than 300 m^2, due to the prominent style of courtyard design within the inner districts of Vienna, with two courtyards being below 1000 m^2 and one courtyard being considerably larger with a total area of over 2000 m^2. All 10 locations are indicated in the map below (Figure 9). Being within a few kilometers from each other, it can be assumed that meso- or synoptic scale climatic conditions are homogeneous, thus not expected to cause differences between the locations. The analysis will focus solely on capturing the microclimatic conditions.

Figure 9: Measurement locations of phase 1 marked on a map (Source: Google Maps - modified)

For the second phase of data collection, 4 geometrically very different courtyards were chosen. The geometric characteristics of these courtyards can be seen in Table 2. Their locations can be seen in in the map below.

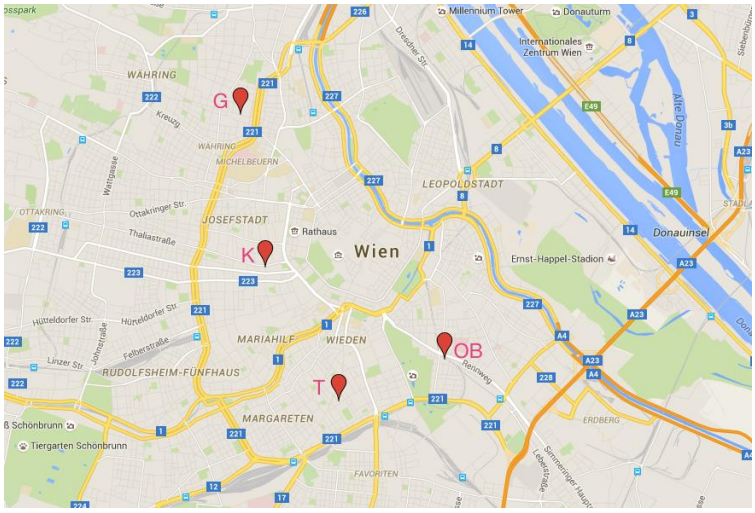

Figure 10: Measurement locations of phase 2 marked on a map (Source: Google Maps - modified)

3.4.1 Location Profiles

The following section describes the 10 courtyards, which were chosen for the first phase of data collection, in more detail. The location of the bicycles is marked by red dots on the maps.

Mozartplatz (M1)

M1 is a small sized courtyard situated at Mozartgasse 4, in the 4th municipal district of Vienna with a total size of 90 $m^{2.}$ With a mean building height of 27.30 m, the built walls fraction is 16.7. This courtyard is fully covered by concrete, building walls and window glass. The courtyard is mainly used for garbage collection and parking. The courtyard at Mozartplatz has the second lowest solar radiation recorded among the 10 locations with values ranging between 4 and 24 W/m^2. The measurements at this location were taken on April 14th 2015, with temperatures around 18 °C.

Figure 11: Courtyard at M1

As can be seen in the map below, M1 is surrounded by buildings on the north and west side, with a main street bordering the houses on the west side. The east and south-east side of the courtyard are closed off to traffic by a square with a fountain and some vegetation. Only the street bordering to the south, Mozartgasse is open for cars but has very low levels of traffic.

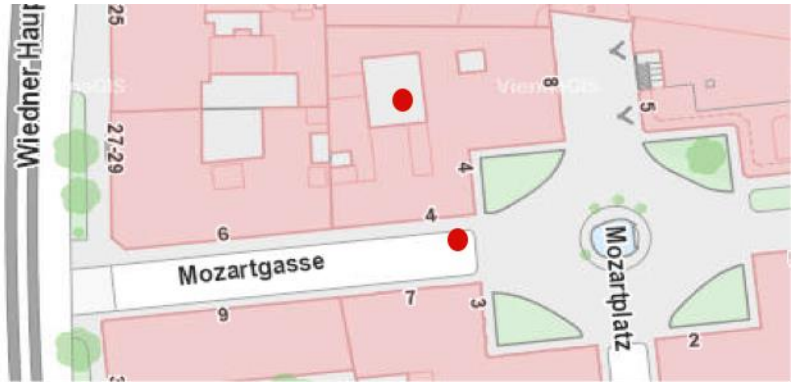

Figure 12: Street Map of M1

Greek Embassy (G1)

The courtyard of the Greek Embassy is also located in the 4th district of Vienna, at Argentinierstraße 16. It is a medium to large sized courtyard with a total area of 620 m^2. With a mean building height of 22 meters, the built walls fraction is 2.15. This courtyard includes some areas covered by soil as well as different types of vegetation such as bush, grass and trees which make up 64% of the total courtyard area. The path in the middle of the courtyard allows for cars to enter, park inside and exit the courtyard. The measurements at this location were taken on April 15th 2015, with temperatures up to 23 °C.

Figure 13: Courtyard at G1

Buildings and other courtyards surround G1 on 3 sides. Only on the east side, there is a relatively large and busy street, Argentinierstraße, which is where the second bicycle was positioned.

Figure14: Street Map of G1

Miesbachgasse 11 (M2)

M2 is a small courtyard with a total area of 90 m^2 and is located in the 2nd district of Vienna, not far from the Danube channel and Augarten, a large recreational park. With a mean building height of 22 meters, the built walls fraction is 7.90. This courtyard does not have any vegetation and is mainly used for garbage collection, bicycle parking and offers a passage between the two buildings sharing the courtyard. Measurements were taken on May 7th 2015, with temperatures up to 23 °C.

Figure 15: Courtyard at M2

As can be seen in Figure 15, the courtyard is surrounded by streets on two sides and by buildings on the other two sides. The bicycle was positioned on Miesbachgasse, close to the building entrance.

Figure 16: Street Map of M2

Paniglgasse (P1)

P1 is a very small courtyard with a total area of 44.5 m^2, located in the city center, just a few meters away from Karlsplatz, one of the main squares of downtown Vienna. With a mean building height of 28 meters, the BWF is one of the highest with 17.49. The courtyard is surrounded by university buildings and is used by smokers. Measurements were taken on April 16^{th,} June 16th and July 1st 2015, with temperatures up to 25 °C.

Figure 17: Courtyard at P1

As can be seen on the map below, there is no vegetation anywhere near the courtyard. While Paniglgasse is a street with rather low traffic, Argentinierstraße, which is the next street to the west, is a rather busy street and might influence the local air quality at Paniglgasse as well.

Figure 18: Street Map of P1

Weyringergasse (W1)

W1 is a medium-sized courtyard with a total area of 180 m^2. There is a small hut in the middle of the courtyard, which most probably serves as sheltered storage space. The average building height is 23 meters and the BWF is 7.41. The courtyard does not have any pervious surfaces and is used mainly as parking space for bicycles and as storage for all kinds of objects. The data was collected on April 23rd 2015, with temperatures up to 21 °C.

Figure 19: Courtyard at W1

As can be seen on the map below, the courtyard is shared between 3 buildings and is surrounded by a main street with considerable amounts of traffic. To the west side, one of Vienna's famous castle parks is located. The area therefore might benefit from the immediate climatic advantages of the park.

Figure 20: Street Map of W1

Schubertring (S1)

S1 is the smallest courtyard with a total area of only 38.5 m^2. The average building height is 28 meters and the H/W ratio is 4.5. This courtyard only serves as space for garbage bins. This type of courtyard is typical for older buildings in the city center of Vienna and usually remains quite cool. The data was collected on May 8th 2015, with temperatures up to 24 °C.

Figure 21: Courtyard at S1

As seen in Figure 21, the courtyard is surrounded by 2 streets. One of them is the Ring, one of the busiest and broadest streets in central Vienna, where the second bicycle was positioned. The street has large trees on both sides and next to it is the Stadtpark, the biggest park in the city center of Vienna.

Figure 22: Street Map of S1

Schikanedergasse (S2)

S2 is medium-sized with 190 m^2. It is the only courtyard, which is enclosed by walls on 3 sides only. With a relatively low mean building height of 15.9 meters, the H/W ratio for this courtyard is 1.9. Covered by soil, grass and two large trees, 47% of the courtyard is made up of pervious surfaces. The measurements at this courtyard were taken on May 12th 2015, when temperatures went up to 25 °C.

Figure 23: Courtyard at S2

As seen on Figure 23, the courtyard is enclosed by other courtyards on two sides and borders a park to the southwest. The adjacent street, where measurements were taken is rather narrow and has very low traffic penetration.

Figure 24: Street Map of S2

Richtergasse (R1)

R1 has a courtyard with a total area of 290 m^2, of which 56% are covered by pervious surfaces, such as grass, bush and a large tree. One of the four walls is covered by ivyleaf. The mean building height is 22 meters and the H/W ratio 1.26. This courtyard is mainly used as passage between the two surrounding buildings and has a restaurant and an office space facing it. The measurements were taken on May 18th and June 4th 2015.

Figure 25: Courtyard at R1

This courtyard is surrounded by a rather narrow street, with very little car traffic. The entrance of the building is faced by a public playground and some trees, as seen on Figure 25.

Figure 26: Street Map of R1

Große Stadtgutgasse (G2)

The courtyard at G2 has 240 m^2 and is covered by 120 m^2 of pervious surfaces such as soil, bush and trees. This courtyard serves as a passage to a second building and as space for bicycle parking. With a mean building height of 20 meters, the H/W ratio for this courtyard is 1.66. The measurements were taken on May 19th 2015.

Figure 27: Courtyard at G2

As can be seen in the map below, the courtyard is made up of two similar sized green areas and a narrow passage in the middle. The building is surrounded by similar buildings with similar courtyards and by the rather large street to the north. This street however does not have a large amount of traffic.

Figure 28: Street Map of G2

Miesbachgasse 15 (M3)

M3 is the largest courtyard with a total area of 2750 m^2. The architecture and size of this courtyard is typical for social housing in Vienna. Tenants enter their apartments from the courtyard. M3 has several trees and some grass areas, with a PSF of 0.75. The H/W ratio is quite low at 0.42.

The measurements at this location were taken on June 5th, with temperatures up to 27 °C.

Figure 29: Courtyard at M3

The courtyard is very large and shared by several houses. One bicycle was positioned right outside the main entrance of M3, while the other bicycle was positioned underneath a tree inside the courtyard.

Figure 30: Street Map of M3

All streets which were compared to the courtyards in phase 1 will be referred to as (Streetcode)_S thereafter (e.g., for location M1, the street will be called M1_S).
For the second phase of data collection, four courtyards were chosen, where the temperature sensors could be attached to the railing of balconies. These courtyards again vary in their geometry and surface characteristics. The geometric factors such as total area, average building height, H/W ratio and PSF can be found in the table 2.

Table 1: Geometric and surface characteristics of 10 courtyards located in Vienna

Location	**Area (m^2)**	**Building Height**	**H/W ratio**	**PSF**
M1	90	27.3	2.4	0
G1	620	22	0.95	0.6
M2	90	22	1.95	0
P1	44.5	28	4.4	0
W1	180	23	1.6	0
S1	38.5	28	4.5	0
S2	190	16	1.9	0.47
R1	290	22	1.26	0.56
G2	240	20	1.66	0.5
M3	2750	24	0.42	0.75

Table 2: Geometric and surface characteristics of 4 courtyards located in Vienna

Location	**Area (m^2)**	**Building Height**	**H/W ratio**	**PSF**
G	1570	27	0.6	0.95
T	845	23	0.7	0.75
OB	3305	25	0.4	0.6
K	49	20	2.9	0

4. RESULTS

The following section shows the main results of the study in form of graphs. The first part shows temperature graphs from the second phase of data collection, with 4 courtyards and their full diurnal cycles (Figures 31 to 35). The second part then shows graphs consolidating all 10 courtyards and adjacent streets and their differences in temperature, absolute humidity, wind and CO_2 during afternoon hours. Morning and evening data is also shown for three separate locations (Figures 36 to 55). The graphs are shown in the same order as they will be discussed in the next chapter. For all the graphs, which show the difference between courtyard and street in terms of a certain parameter, the following equation was used:

$$\Delta P = V(c) - V(s) \qquad (10)$$

Where ΔP is the difference in parameter (for example temperature), $V(c)$ is the parameter value inside the courtyard and $V(s)$ is the parameter value at the street level.

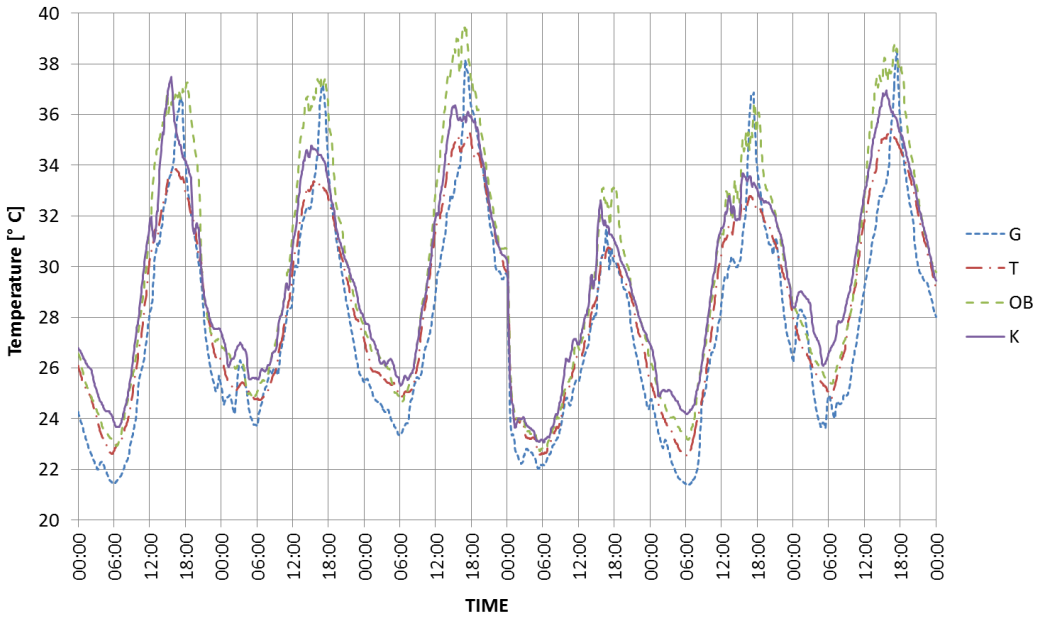

Figure 31: Diurnal cycle of temperature of courtyard measured at 4 locations between July 18th and July 22nd 2015

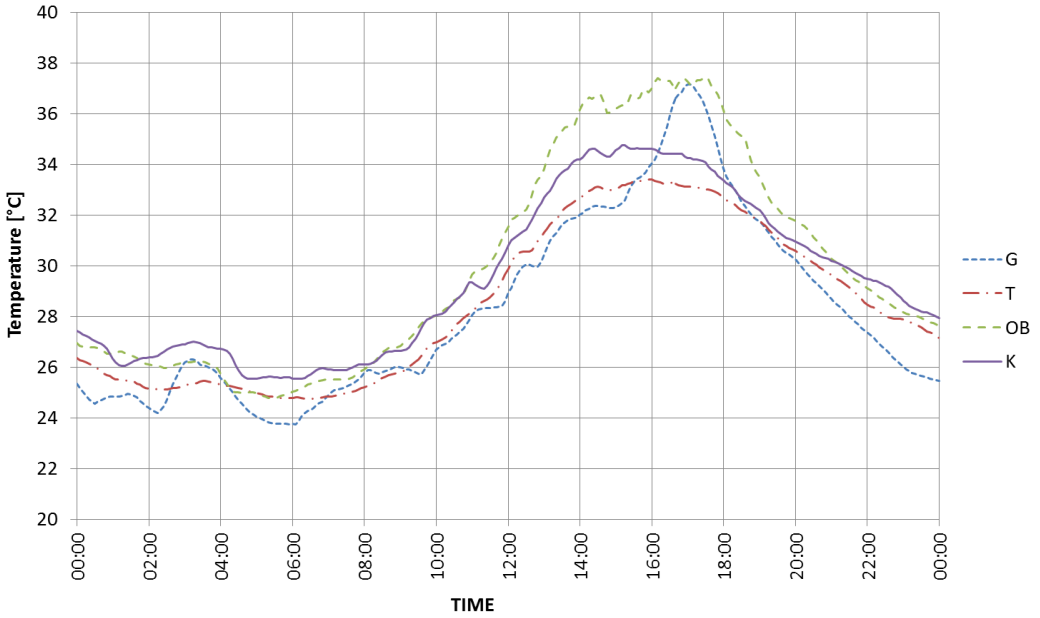

Figure 32: Temperature of courtyards measured at 4 locations over a period of 24 hours on July 18th 2015

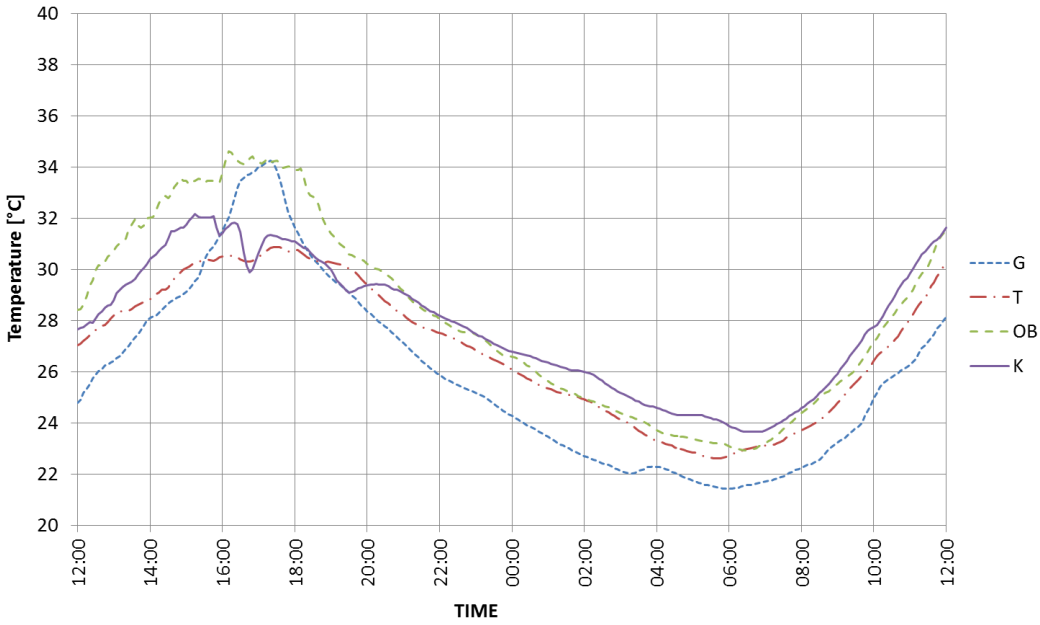

Figure 33: Temperature of courtyards at 4 locations as a function of time measured for a period of 24 hours (12:00 to 12:00) on July 16th and 17th 2015

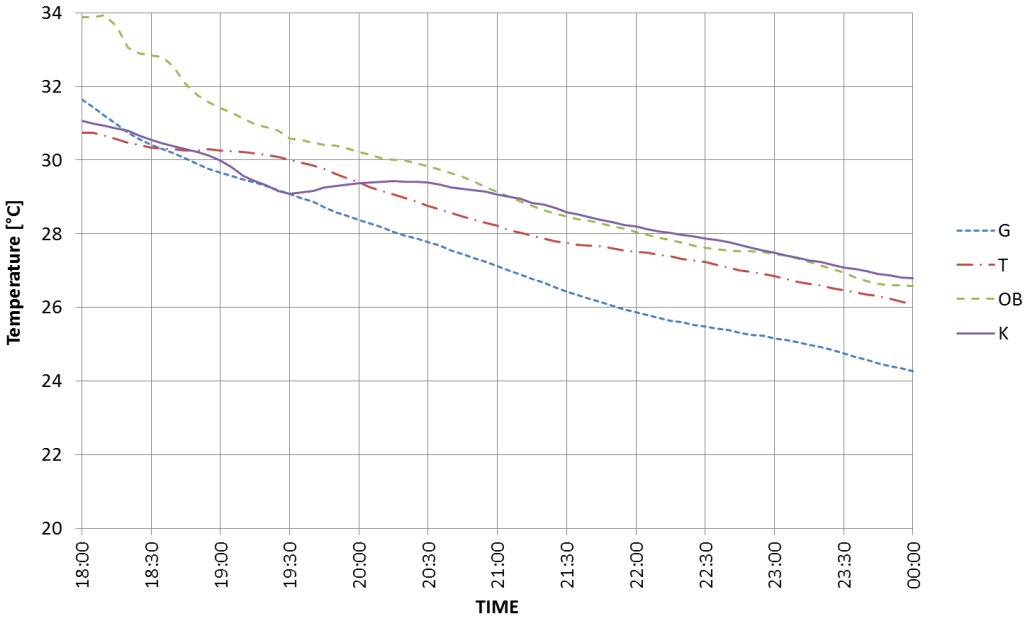

Figure 34: Temperature of courtyard at 4 locations as a function of time measured during evening hours (18:00-24:00) on July 16th 2015

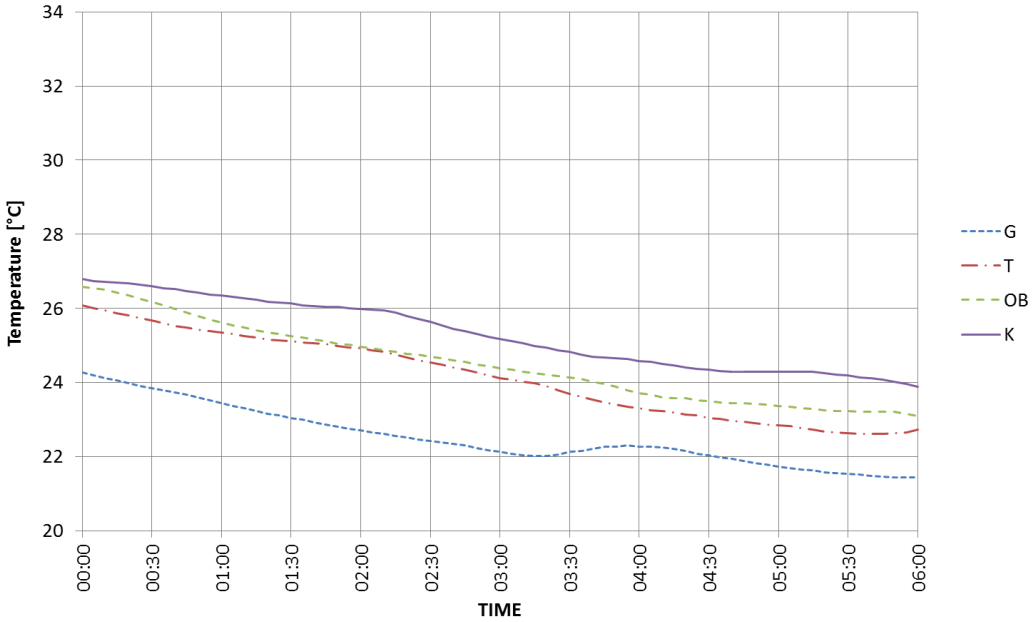

Figure 35: Temperature of courtyards measured at 4 locations as a function of time measured during night time (00:00 – 06:00) on July 17th 2015

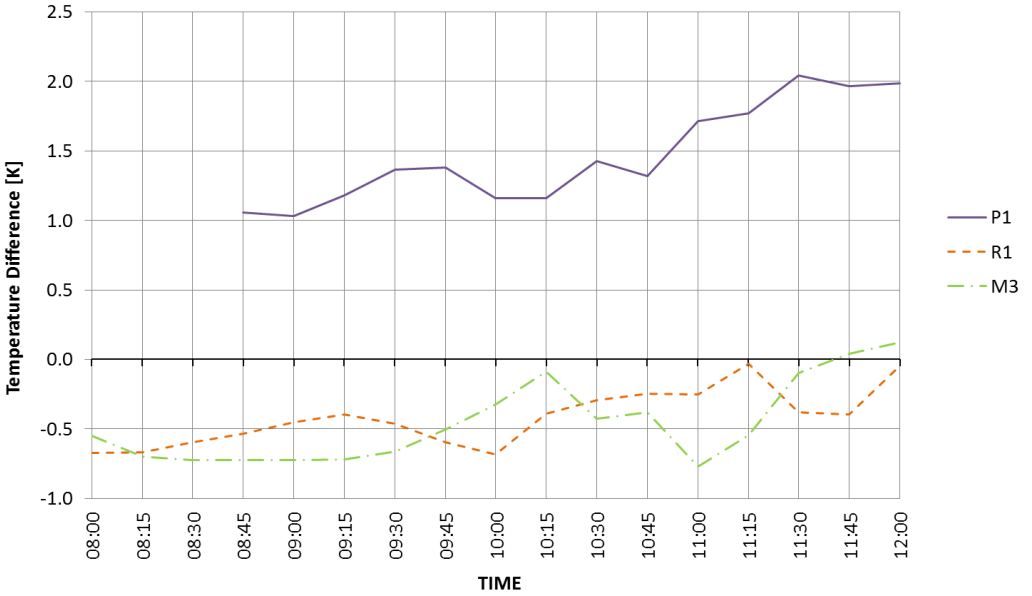

Figure 36: Temperature difference between courtyard and street for 3 locations as a function of time of the day (measured on different days during morning hours (08:00-12:00) in June 2015).

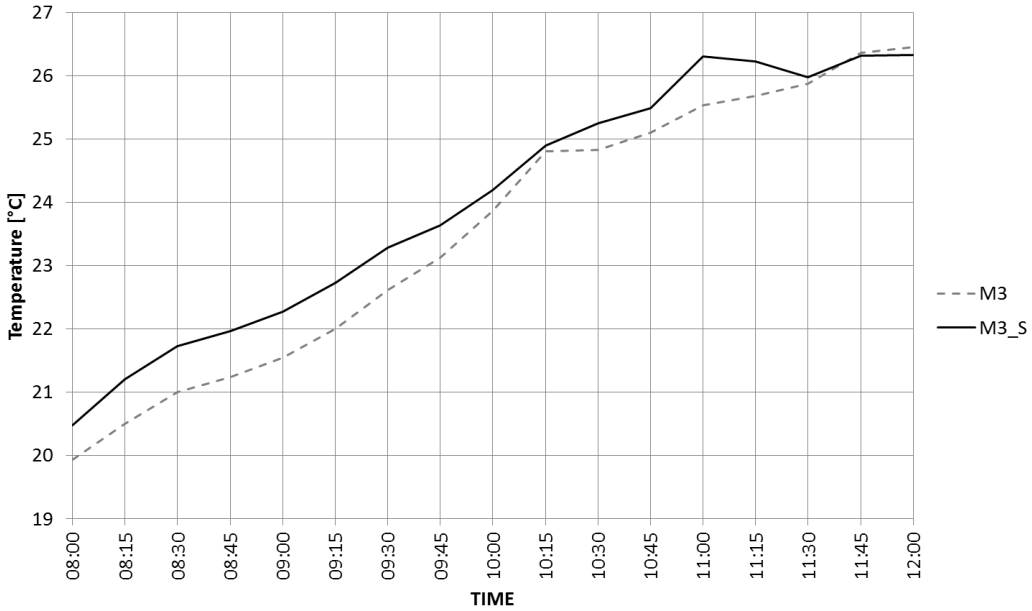

Figure 37: Temperature of courtyard (M3) and street as a function of time measured during morning hours (08:00-12:00) on June 5th 2015

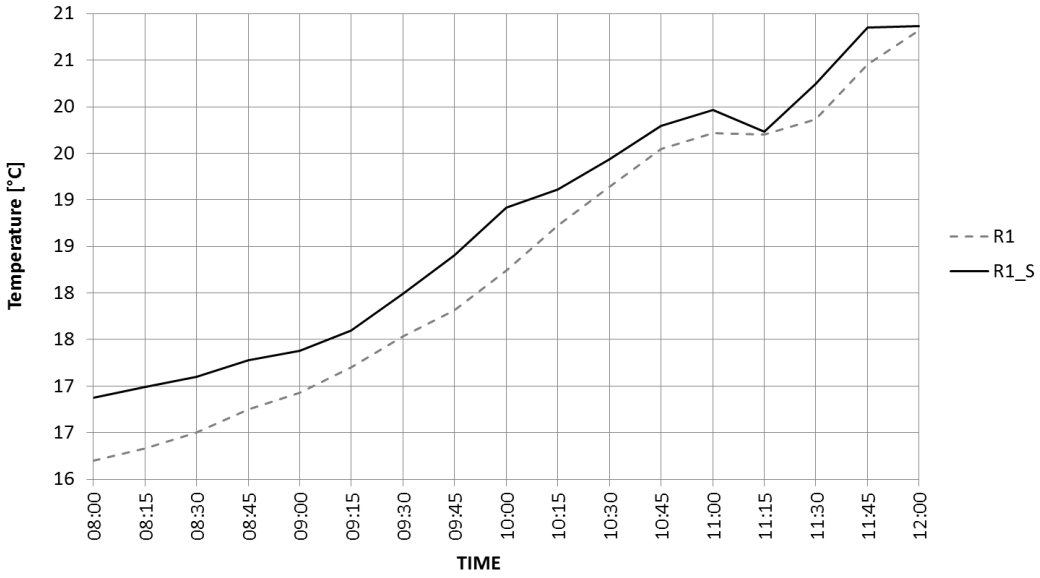

Figure 38: Temperature of courtyard (R1) and street as a function of time measured during morning hours (08:00-12:00) on May 18th 2015

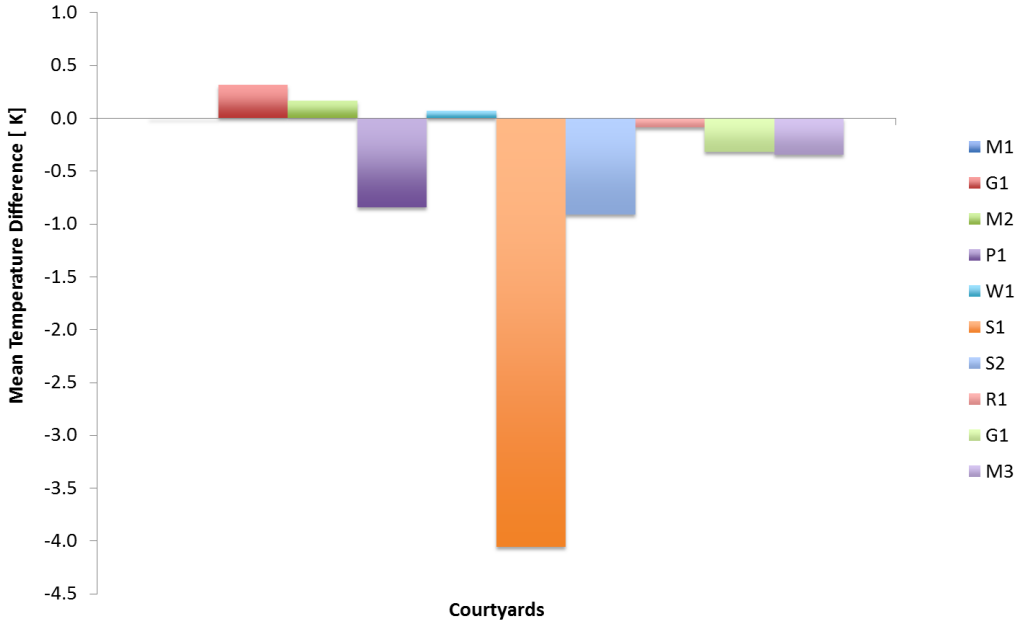

Figure 39: Mean temperature difference between courtyards and street at 10 different locations measured at afternoon hours (13:00 – 17:00) during the period of April and July 2015

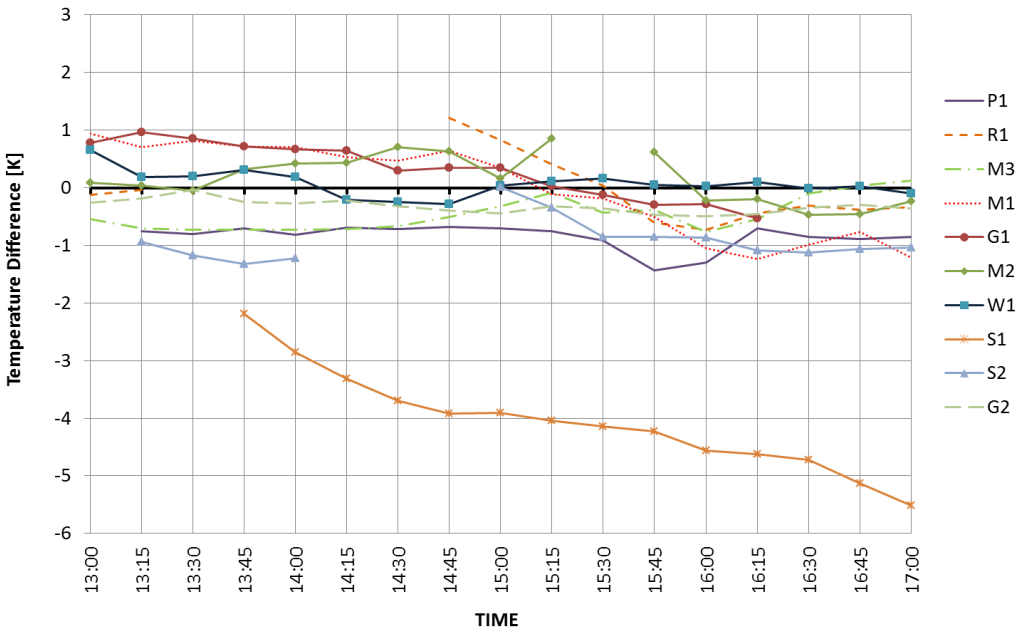

Figure 40: Temperature difference between courtyard and street at 10 locations as a function of time of the day (measured on different days during the period of April until July 2015)

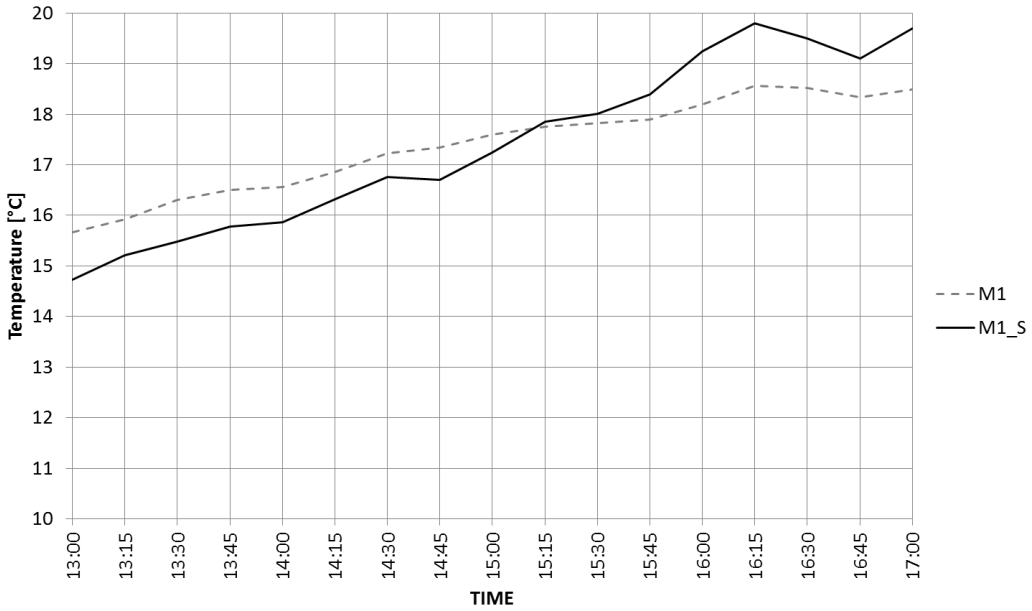

Figure 41: Temperature at courtyard (M1) and street as a function of time of the day measured during afternoon hours (13:00-17:00) on April 14th 2015

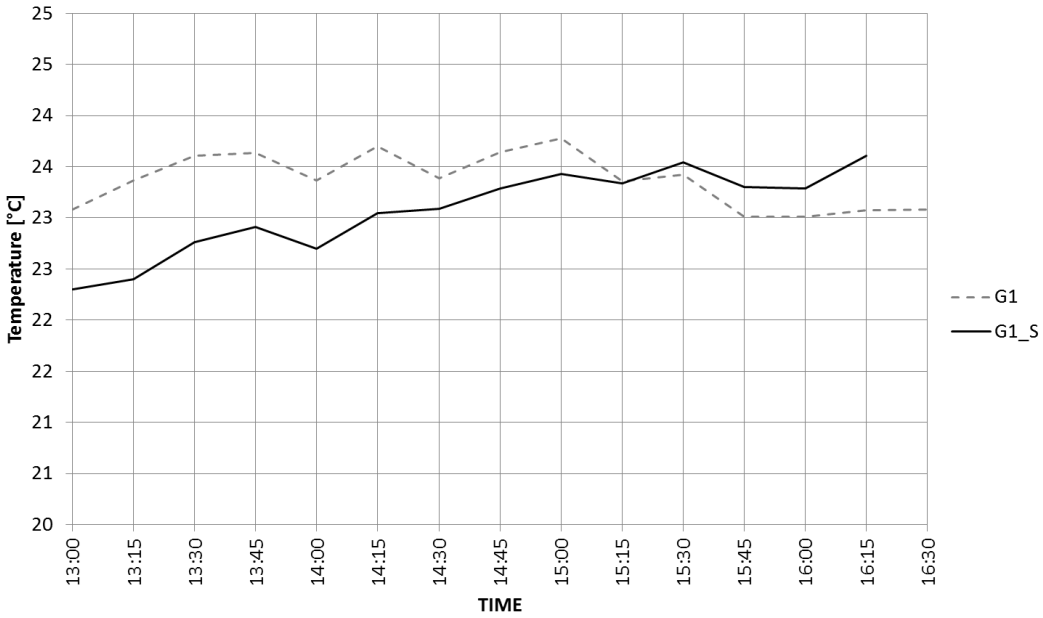

Figure 42: Temperature at courtyard (G1) and street as function of time of the day measured during afternoon hours (13:00 -17:00) on April 15th 2015

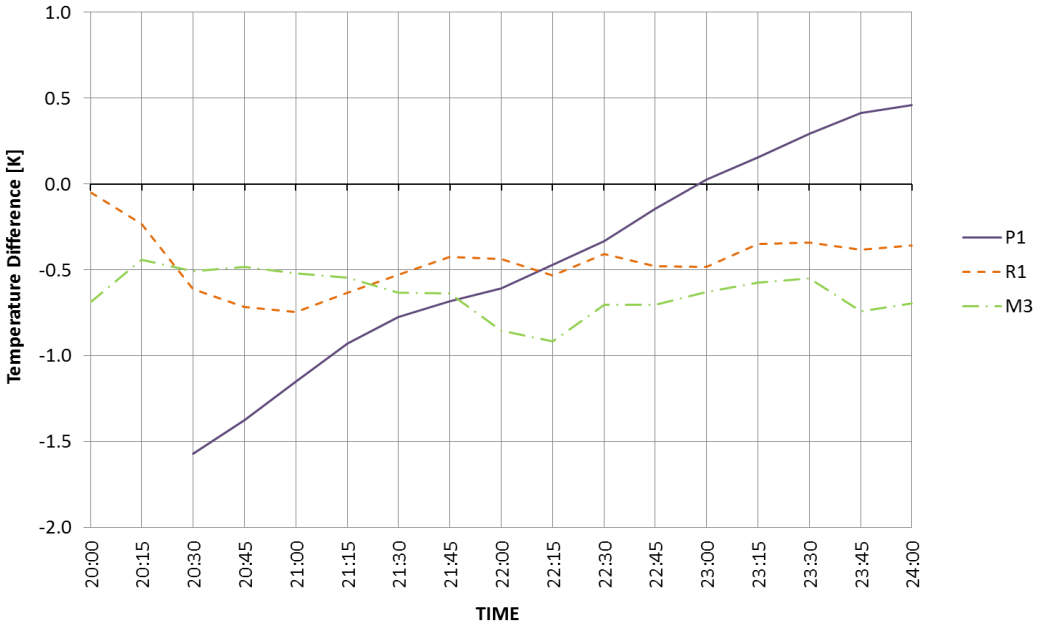

Figure 43: Temperature difference between courtyard and street for 3 different locations as a function of time of the day measured at night (20:00-24:00) on different days in June 2015

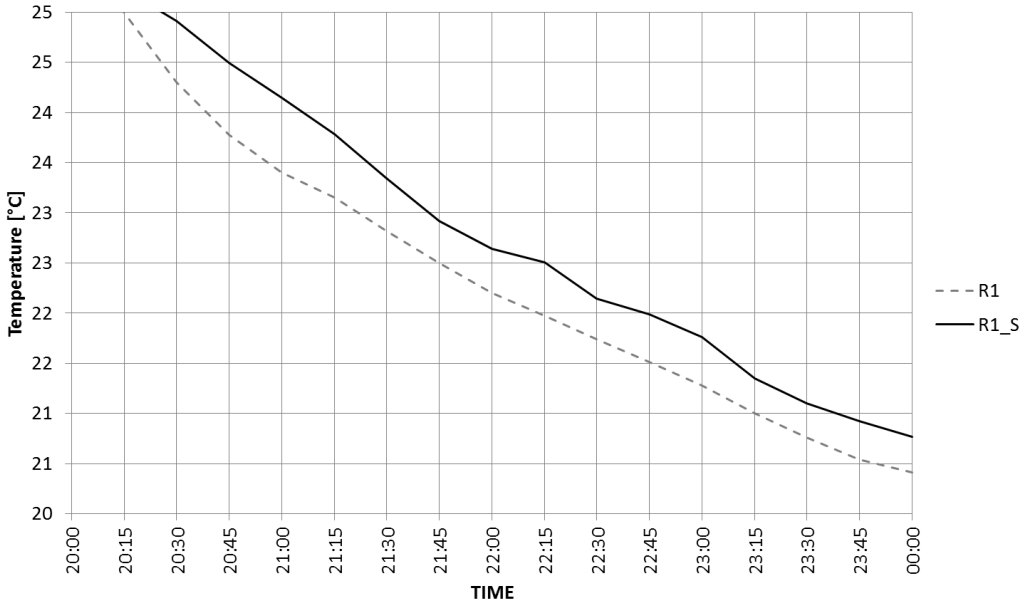

Figure 44: Temperature of courtyard (R1) and street measured as a function of time of the day during night (20:00 – 24:00) on June 4th 2015

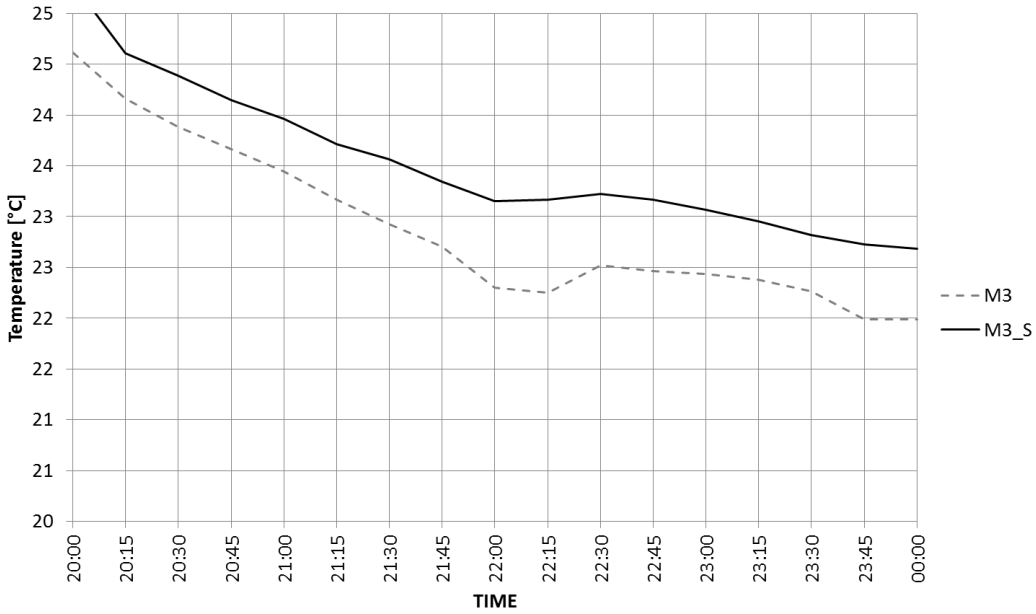

Figure 45: Temperature of courtyard (M3) and street measured as a function of time of the day during night (20:00 – 24:00) on June 5th 2015

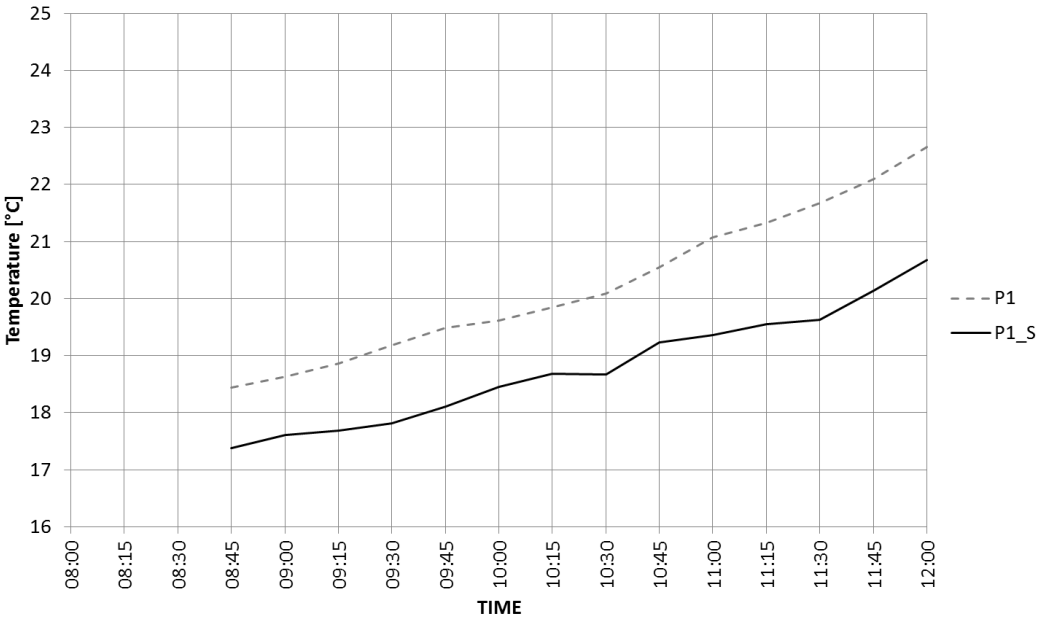

Figure 46: Temperature of courtyard (P1) and street as a function of time measured during morning hours (08:00-12:00) on June 16th 2015

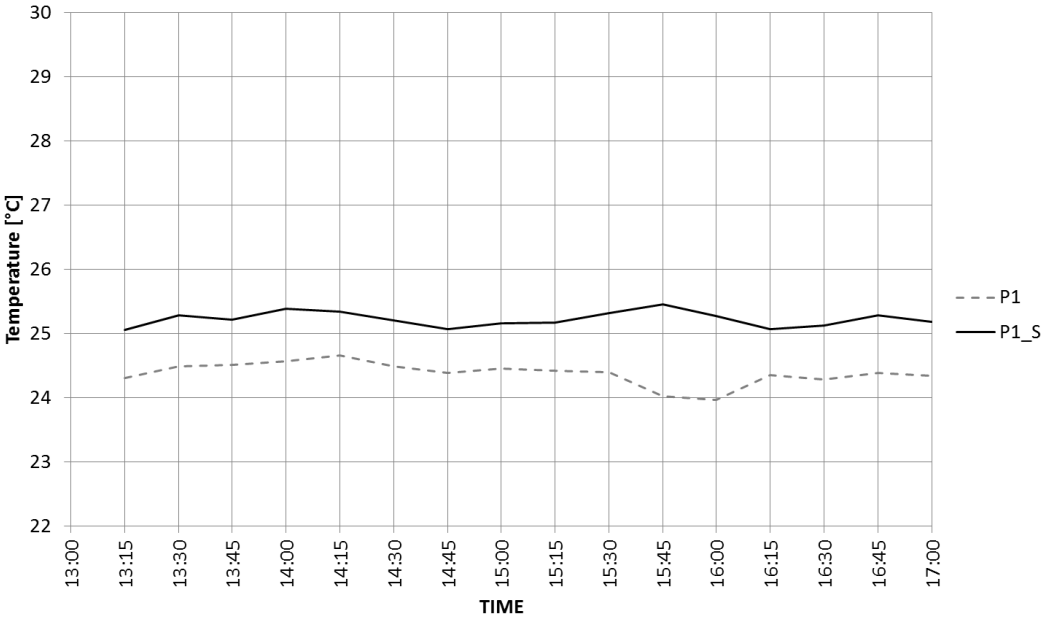

Figure 47: Temperature of courtyard (P1) and street as a function of time measured during afternoon hours (13:00-17:00) on April 16th 2015

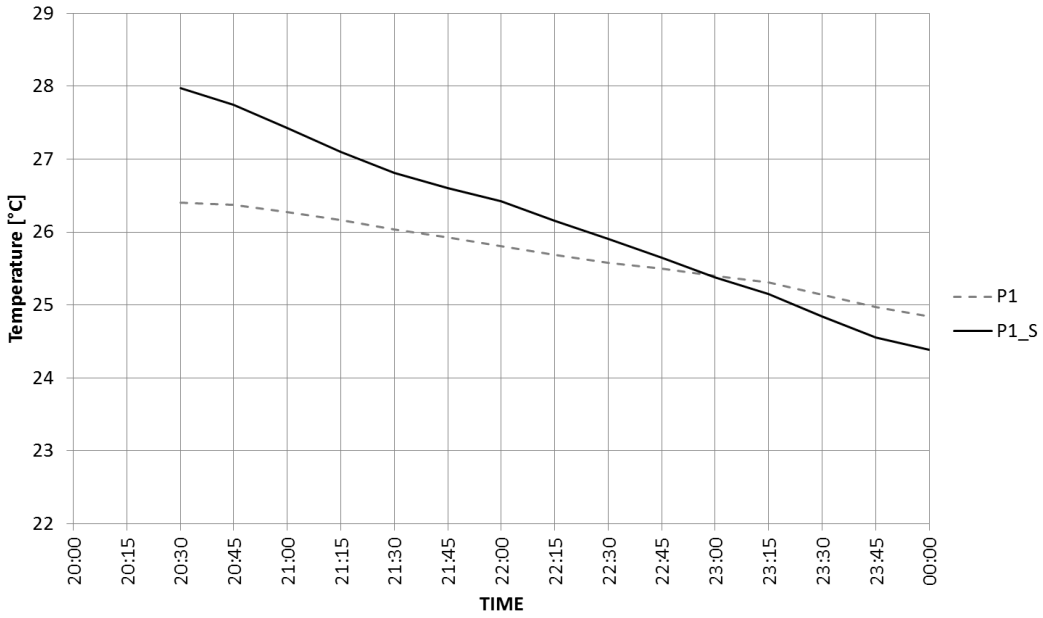

Figure 48: Temperature of courtyard (P1) and street as a function of time measured during night hours (20:00-24:00) on July 1st 2015

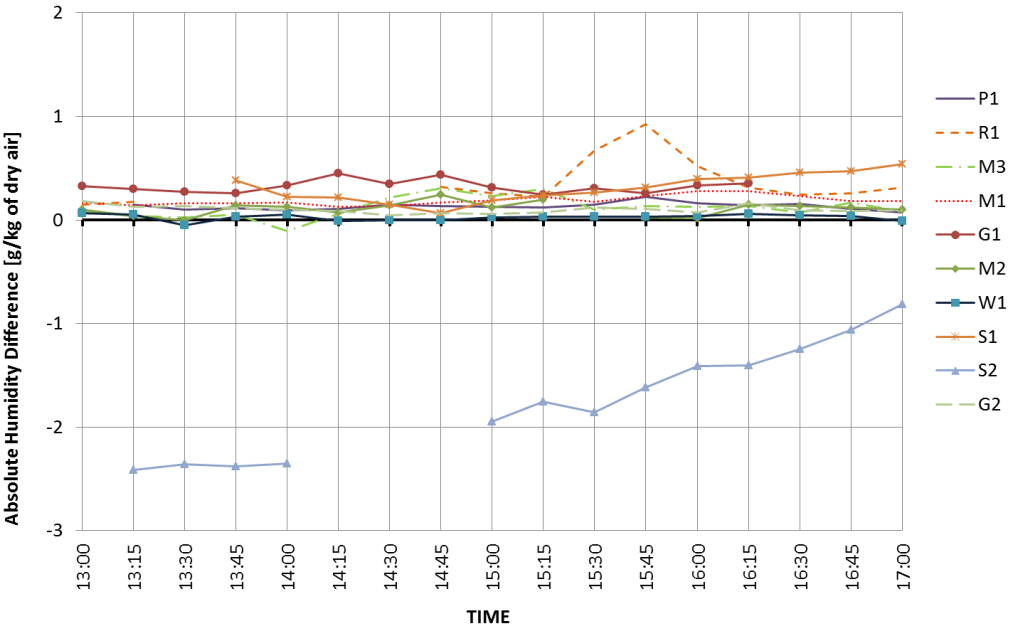

Figure 49: Absolute humidity difference between courtyard and street at 10 locations measured during afternoon hours (13:00-17:00) on different days between April and July 2015

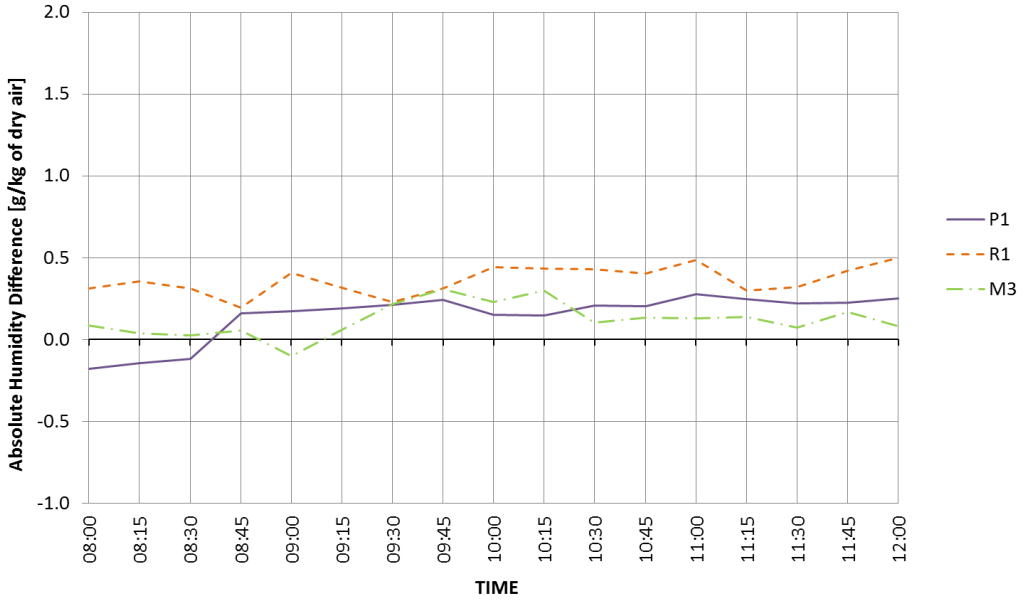

Figure 50: Absolute humidity difference between courtyard and street at 3 locations measured during morning hours (08:00-12:00) on different days between June and July 2015

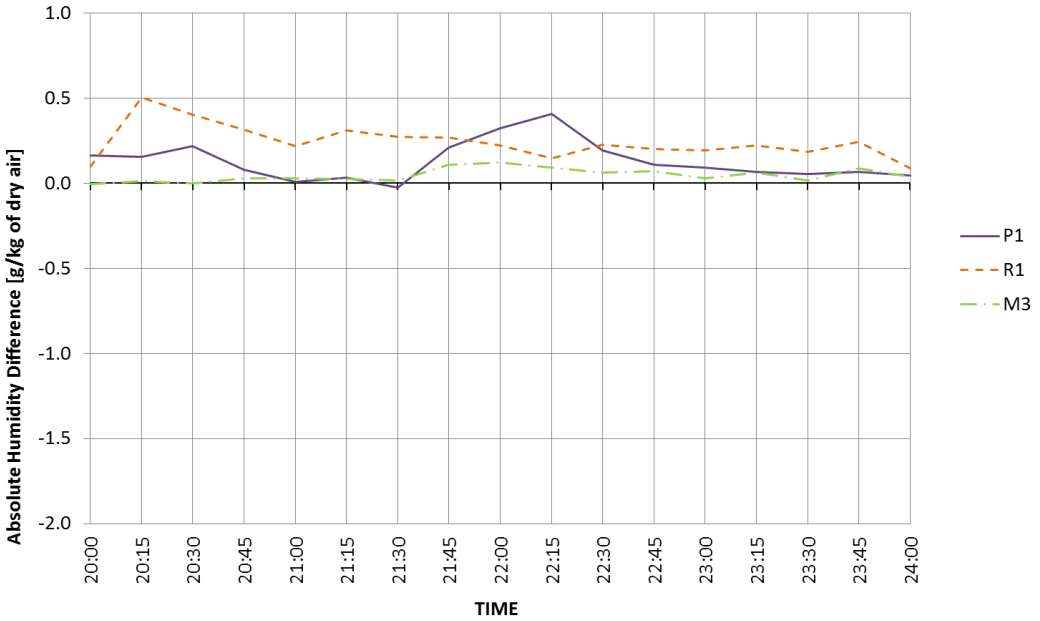

Figure 51: Absolute humidity difference between courtyard and street at 3 locations measured during night hours (20:00-24:00) on different days between June and July 2015

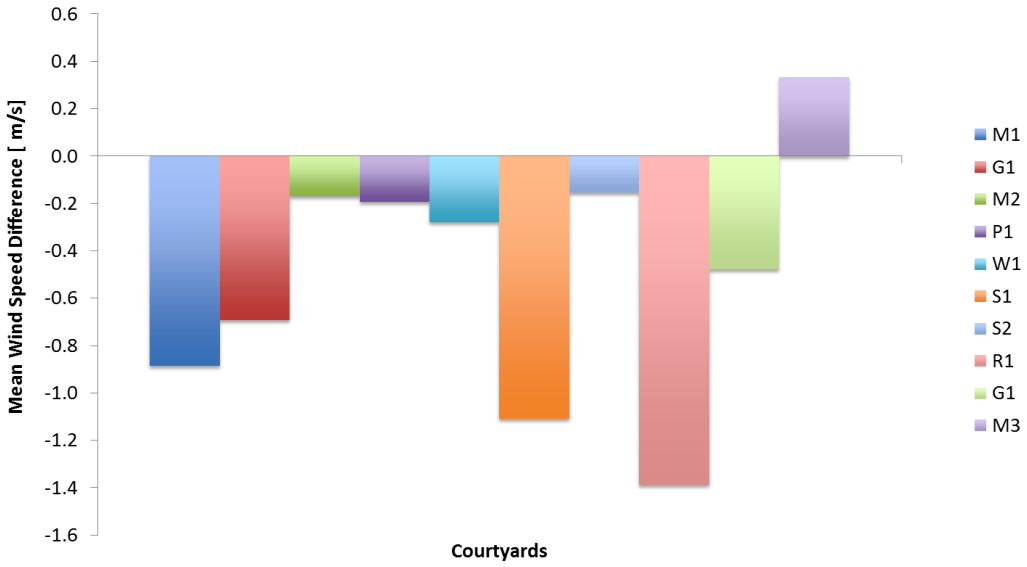

Figure 52: Mean wind speed difference between courtyards and street at 10 different locations measured at afternoon hours (13:00 – 17:00) during the period of April and July 2015

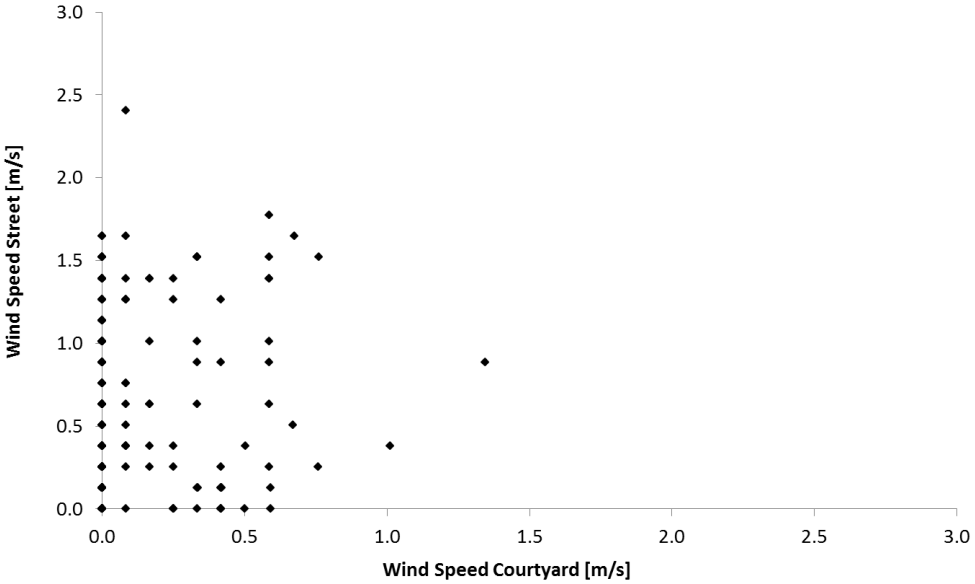

Figure 53: Mean wind speed in courtyard versus street at 10 locations measured in the afternoon hours (13:00-17:00) between April and July 2015

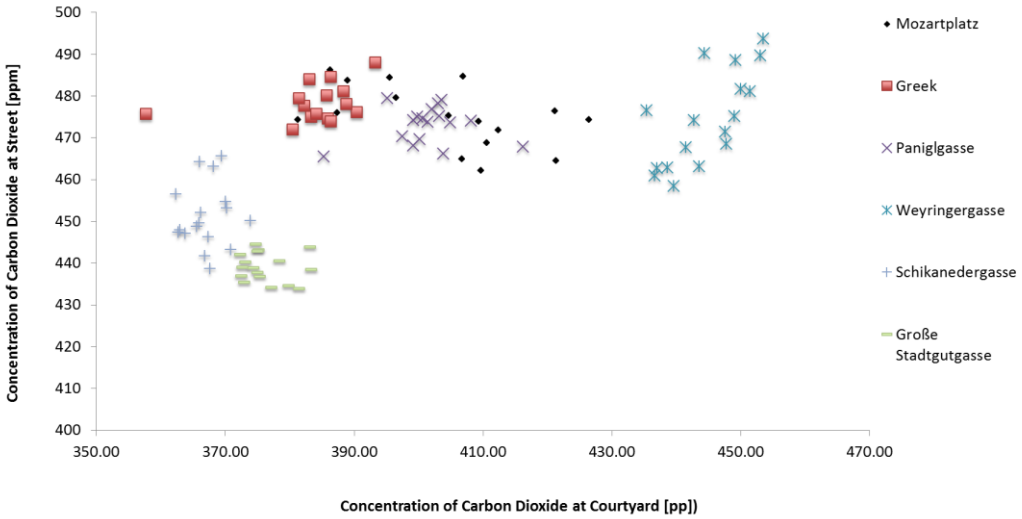

Figure 54: Scattered plot of Carbon Dioxide concentrations in courtyard versus street measured at 6 locations during afternoon hours (13:00 – 17:00) between April and July 2015

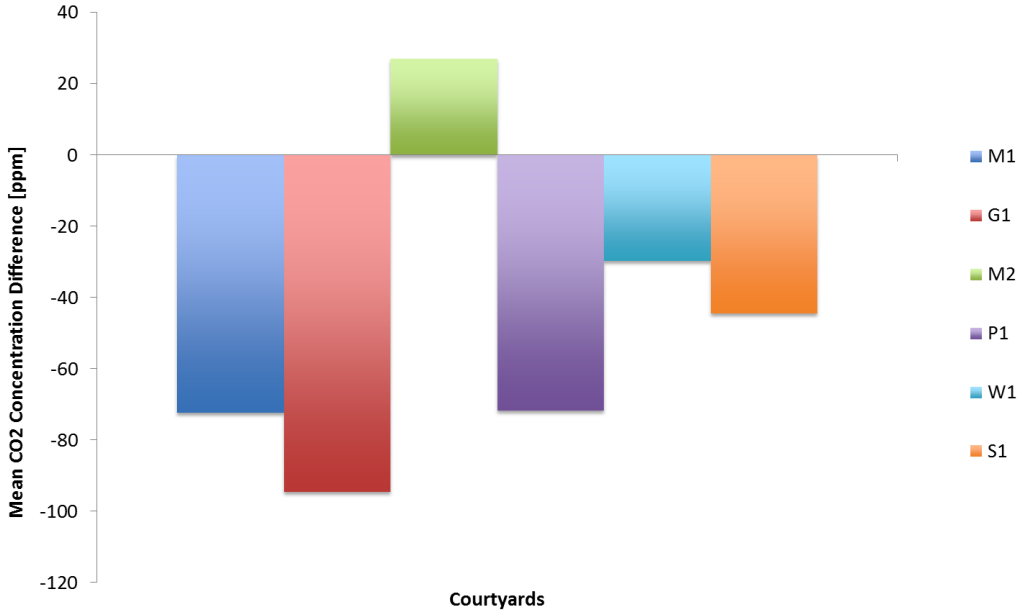

Figure 55: Difference in concentration of Carbon Dioxide between courtyard and street measured during afternoon hours (13:00 – 17:00) at 6 locations between April and July 2015

5. DISCUSSION

This chapter discusses the main findings of this study with the help of data provided in the form of graphs. First, general findings about the thermal behavior of courtyards will be made. For this analysis the temperature data from the second phase of data collection was used, where full diurnal cycles were recorded simultaneously and hence different types of courtyards could be compared to each other. The second part of the discussion will then focus on the first phase of data collection, presenting the main findings where courtyards and streets were compared for temperature, absolute humidity, wind and CO_2.

5.1 Courtyards

As noted in several previous studies, the building geometry of courtyards may have a decisive effect on its thermal behavior. As such, the H/W ratio is one of the parameters, which are expected to have some influence on the air temperature inside the courtyard throughout a full diurnal cycle (Meir 1995). Courtyards with a high H/W ratio can be expected to generally heat up less during the day but cool off less effectively during the night. This phenomenon can be observed in Figure 31, which shows 5 consecutive diurnal cycles at 4 different courtyards. The courtyard with the highest H/W ratio, K, shows the smallest variance in temperature. During noon and afternoon hours, when air temperatures reach their peak, K heats up around 2-4 K less than the open and very large courtyards, G and OB. On the other hand, it does not cool down as effectively and remains the hottest during the night, with similar temperature differences of 2-4 K. Two different effects may explain such distinct thermal behavior. During afternoon hours, less sunlight is able to penetrate into the courtyard compared to more open courtyards; a courtyard with a higher H/W ratio may therefore heat up less during the day. During nighttime such a courtyard may however not cool down as effectively, due to the back radiation by urban surfaces, which is trapped inside the courtyard by the higher fraction of building walls available.

Courtyards with a more open geometry, such as courtyards that are open to one side or courtyards with very low H/W ratios, are expected to have better ventilation due to their specific geometry. These spaces may cool down more effectively over night. This behavior can also be observed in Figure 31, which shows that G, a courtyard enclosed on 3 sides only, cools down more effectively than the other courtyards on 5 consecutive nights.

Courtyards, irrespective of their geometric features, start to heat up from 06:00 onwards and usually reach their peak temperatures in the early afternoon hours. This can be observed in Figure 32, which shows a typical diurnal cycle at the same 4 locations. From around 17:00 they start cooling down. Most of the cooling down takes place in the late evening hours (18:00 and 24:00) (Figure 33). While all courtyards continue to cool down until 06:00, the rate of temperature drop between 24:00 and 06:00 is slower as compared to the interval of 18:00-24:00. This can be seen when comparing the curves of Figures 34 and 35. The temperature drop in the first 6 hours ranges between 4 and 7 K, while thereafter each of the 4 locations cools no more than 2-3 K until sunrise, when they start heating up again.

5.2 Comparing courtyards and streets

For this analysis, data collected at 10 different locations was used for afternoon hours (13:00-17:00) and data from 3 locations was used for morning and evening hours. This section is divided into comparing remarks between courtyards and streets in terms of temperature, absolute humidity, wind and CO_2 and tries to account for deviations, which were found during data collection.

5.2.1 Temperature

In the morning, both street and courtyard start heating up (Figure 36). Generally, courtyards remain slightly cooler than the street during morning hours (08:00 – 12:00). The outlier at P1 will be explained as a special case in more detail towards the end of this chapter.

While both street and courtyard heat up during morning hours, courtyard temperatures increase at a slightly higher rate. This leads to the courtyard temperatures catching up with the street around noon. This phenomenon can be observed in Figures 37 and 38. Both courtyards, R1 and M3, while very different in size, have a relatively low H/W ratio of 1.26 and 0.42 respectively. This may explain a compromised shading effect by the building walls during late morning hours and early noon, when the sun is at its highest.

During afternoon hours (13:00-17:00), courtyards are generally cooler than the street. The results in Figure 39 show that in 6 out of 10 cases, courtyards are on average cooler during afternoon hours, of which in 3 cases the courtyards are significantly cooler. Between 13:00 and 15:00 most courtyards are hotter than the street. This trend is then reversed (Figure 40). Since measurements were only done between 08:00 and 12:00 and 12:00 and 17:00, there is no data available for the timeframe of 12:00 to 13:00. Knowing that courtyards are generally cooler than the street during morning hours, but hotter than the street after 13:00, we can assume that the courtyard temperature exceeds the street temperature between 12:00 and 13:00.

After 15:00 all courtyards start to cool off at least relatively to the street. This reversal can be observed in Figures 41 and 42, where both M1 and the G1 show, that the courtyard is exceeding the street temperature until approximately 15:00, when the street becomes hotter than the courtyard in both cases. This behavior may again be explained through the shading effect, which is less effective during noon hours, when solar radiation can penetrate more freely into the courtyard. Simultaneously, more heat may be absorbed and retained in the courtyards, since more building surface is available compared to street canyons. Furthermore air is more stagnant in an enclosed area, which can have a compromising effect on heat removal through air exchange. This aspect will be explained further in the analysis of wind speeds.

During evening hours, both street and courtyards start cooling down in a similar way. Streets however remain hotter than the courtyards (Figure 43). Here again, P1 displays a different relationship between street and courtyard, which will be

analyzed separately. As seen in Figures 44 and 45, courtyard temperatures remain constantly below street temperatures until midnight. While data for the late night hours are missing, it can be assumed that courtyards remain cooler than the street for the entire night, since the morning measurements showed that courtyards were still cooler than the street from 08:00 onwards.

P1 : A special case

P1, compared to all other locations of the second phase of data collection, has the highest H/W ratio (4.37) as well as the highest building walls (28 meters). Both these geometric factors can have a decisive impact on the thermal conditions inside a courtyard (Almafdy et al. 2013). Furthermore such courtyards seem to behave differently in relation to the street as compared to the temporal cycle previously explained.

Courtyards with higher H/W ratios seem to be hotter than the street during morning hours (Figure 46). This might be the case, because of the slower cooling rate during the night.

During early afternoon hours however, they seem to heat up less than the street (Figure 47). While data between 12:00 and 13:00 is missing, the courtyard at P1 is considerably cooler for the entire afternoon measurement period, which means that the street temperature must exceed the courtyard temperature sometime between 12:00 and 13:00. This phenomenon could possibly be explained by a more pronounced shading effect by the high courtyard walls. A study performed by Almafdy et al. in 2013 showed that an increasing number of floors, i.e. the height of the building could decrease air temperature inside the courtyard. Similarly, the courtyard at P1, may be exposed to fewer hours of direct incoming solar radiation as compared to the street canyon, due to its high walls and high H/W ratio.

During evening hours, when both street and courtyard start to cool down, the temperature curve of the courtyard can be expected to be flatter than the street, since the courtyard might not cool off as effectively as the street (Figure 48). The street is hence expected to become cooler than the courtyard, which was recorded to happen at around 23:00 at P1. This phenomenon might be explained through

the trapping of heat, which is re-emitted by the building walls in form of long-wave radiation. Courtyards with high H/W ratios hence cool off less effectively due to their restricted long-wave radiative potential (Meir 1995).

5.2.2 Humidity

Courtyards are as humid or slightly more humid than their adjacent street canyons. This relationship can be well observed in Figure 49. With humidity values ranging between 3 to 8 g/kg of dry air, they remain more humid than the street throughout evening as well as morning hours (Figures 50 and 51). There are several plausible explanations for these findings. Firstly, the expected lower air exchange rates (explained in the next section on wind speeds) within courtyards could cause for a greater part of the moisture to remain inside them.

Secondly, the usage of water and the water content inside buildings may lead for building walls to emit some of that moisture into the courtyard.

Thirdly, we would expect that the presence of vegetation and unsealed surfaces could increase humidity values due to an increased ability to absorb and re-emit moisture through evapotranspiration. The data however shows, that both courtyards with and without vegetation and sealed surfaces are similarly more humid than their street counterpart. This might point toward the other two effects being more pronounced.

As seen in Figure 49, there is only one location (S2), which is considerably drier than the street. S2 is the only courtyard out of the 10 chosen locations, which is enclosed by walls on 3 sides only. The therefore resulting higher ventilation rate might explain part of this behavior. However, it cannot offer a full explanation.

5.2.3 Wind

According to Meir (1995), air movement inside courtyards is important for human comfort in two ways: firstly in a direct way, in form of air flow in contact with the skin and secondly in form of advection of hotter or colder air from outside the courtyard. Depending on the geometry of the courtyard itself as well as on the

building density of the surrounding blocks, different wind regimes have been previously quantified. For example, consecutive building blocks with a H/W ratio of 0.65 or more have a decisive effect on the wind patterns reaching into street canyons and courtyards. Such areas may be considered to be sheltered from direct impact of winds. Winds at ground level are hence weak, which results in compromised ventilation inside the courtyards. While this effect may impact residents negatively during hot summer months, this same phenomenon can be considered as being positive during cold, windy winter months.

In accordance with previous findings, this study showed that wind speeds inside courtyards are lower than at street level in 9 out of 10 cases, with wind speeds inside the courtyard being about half of the speed at the street (Figures 52 and 53). The courtyard geometry can be thought to act as an obstruction in the general airflow pattern. The only exception in this series is M3, which is the largest courtyard, as well as the courtyard with the lowest H/W ratio of 0.42. Being the only courtyard with a H/W ratio lower than 0.65, it is also located very close to a large park, and hence surrounded by a lower building density, that is usual for most buildings in the inner districts of Vienna.

5.2.4 CO_2

The recorded CO_2 values were found to be lower inside courtyards during daytime (Figure 55). Values range between 350 and 460 ppm inside courtyards and between 420 and 490 ppm at street level (Figure 54).
The reason for lower CO_2 levels inside courtyards may again be related to the compromised airflow between other urban spaces and courtyards themselves. The air from streets, with higher increased CO_2 levels due to car traffic, cannot reach or completely mix into the courtyard air.

6. CONCLUSION

6.1 Contribution

This study has shown the thermal behavior of courtyards in general over full diurnal cycles as well as specific differences between courtyards due to their specific geometric properties. Courtyards with high building walls and a high H/W ratio seem to behave differently from more open courtyards, in that they remain somewhat cooler during the day but cannot cool down as effectively over night.

Compared to their adjacent street canyons, courtyards seem to be generally cooler, except during noon and afternoon hours, when the sun is at its highest position.
With these results in mind, courtyards have climatic benefits for city dwellers; since they are generally cooler, display slightly higher humidity values and lower CO_2 concentrations.

From the data collected, we can deduce that small courtyards with high building walls can create disadvantageous thermal conditions during summertime, especially during morning and evening hours, which is when most people would be expected to make use of courtyard spaces. During wintertime, such geometry may be equally problematic due to an even smaller proportion of sun radiation being able to penetrate into the courtyard. It would hence be recommended to keep H/W ratios low, so that enough solar radiation may penetrate into the courtyard during cold winter months, as well as to guarantee proper ventilation during hot summer months.

Finally, although not the strongest parameter in influencing the overall human comfort in a courtyard, having non-sealed surfaces inside courtyards can allow for humidity to be absorbed and stored for delayed evapotranspiration. While trees inside courtyards do not seem to influence the overall air temperature to a decisive extent, they may still serve to give shadow to people spending time in courtyards.

6.2 Future Research

This research has shown interesting first insights into the specific thermal conditions of different types of courtyards and their adjacent streets. To determine their significance in effectively mitigating the urban heat island effect, further research is of vital importance.
Since this work has concentrated on the city of Vienna, it would be important to conduct similar research in cities with more extreme climatic conditions, where the effect and its consequences can be expected to show an amplification.
Similarly, it would be interesting to extend the research into winter months, to see how design variants, which are advantageous over the summer behave thermally during cold weather.

Furthermore, being aware of the restriction of time and resources, further data collection is necessary to make definite mitigation suggestions. First steps would be to collect data several times at the same locations, in order to be able to analyze the thermal behavior of each location under different weather conditions. Secondly, with the necessary resources, data could be collected simultaneously at all locations in order to be able to directly compare all of them.

In the course of this work, for equipment security reasons, full diurnal cycles could only be recorded within courtyards but not on the street, hence the acquisition of such data is of prime interest for further research.

List of References

Akbari, H., Pomerantz, M., Taha, H. (2001): Cool surfaces and shade trees to reduce energy use and improve air quality in urban areas. Solar Energy 70, 295-310

Alexandri, E and Jones, P. (2008): Temperature decreases in an urban canyon due to green walls and green roofs in diverse climates. Building and Environment 43, 480-493

Ali-Toudert, F. and Mayer, H. (2006): Numerical study on the effects of aspect ratio and orientation of an urban street canyon on outdoor thermal comfort in hot and dry climate. Building and Environment 41, 94-108

Almafdy, A., Ibrahim, N., Ahmad, S. and Yahya, J. (2013): Courtyard Design Variants and Microclimatic Performance. Social and Behavioral Sciences 101, 170-180

Conti, S., Meli, P., Minelli, G., Solimini, R., Toccaceli, V., Vichi, M., Beltrano, C. and Perini, L. (2005): Epidemiologic study of mortality during summer 2003 heat wave in Italy. Environmental Research 98, 390-399

CCOHS (2015): Humidex Rating and Work. http://www.ccohs.ca/oshanswers/phys agents/humidex.html - accessed on February 10th

Dessì, V. (2011): Urban materials for comfortable open spaces. Sustainable Cities and Regions, World Renewable Energy Congress, May 2011

Dimitrova, B. (2013): Urban Heat Island and Mitigation Strategies for case study Vienna. Diploma thesis. Vienna University of Technology, Vienna.

Epstein, J and Moran, D. (2006): Therman Comfort and the Heat Stress Indices. Industrial Health 44, 388-398

Gartland, L. (2011): Heat Islands: Understanding and Mitigating Heat in Urban Areas. Earthscan, London

Hammerberg, K. and Mahdavi, A. (2014): GIS-based simulation of solar radiation in urban environments. In: Mahdavi, A., Martens, B. and Scherer, R.: eWork and eBusiness in Architecture, Engineering and Construction, CRC Press, Netherlands, 2243-2250

Hanner, M.S., Giese, R.H., Weiss, K. and Zerull, R. (1981): On the definition of Albedo and Application to Irregular Particles. Astronomy and Astrophysics, 106, 42-46

Hoboware (2015): Graphing and Analysis Software http://www.onsetcomp.com/products/software/hoboware - accessed on February 9, 2015

Karlessi, T., Santamouri, M. and Synnefa, A. (2009): Thermochromic energy efficient coatings for buildings and urban structures. http://heatisland2009.lbl.gov/docs/211530-karlessi-doc.pdf - accessed on September 18, 2015

Kleerekoper, L., van Esch, M. and Baldiri Salcedo, T. (2012): How to make a city climate-proof, addressing the urban heat island effect. Resources, Conservation and Recycling 64, 30-38

Krätschmer, E. (2010): Implication of urban heat island for architecture. Diploma thesis. Vienna University of Technology, Vienna.

Laaidi, M., Zeghnoun, A., Dousset, B., Bretin, P., Vandentorren, S., Giraudet, E. and Beaudeau, P. (2012): The impact of heat islands on mortality in Paris during the August 2003 heat wave. Environmental health perspectives 120, 254-259

Li, H., Harvey, J., Holland, T. and Kayhanian, M. (2013): The use of reflective and permeable pavements as a potential practice for heat island mitigation and stormwater management. Environmental Research Letters 8

Lobo, C. (2015): Cool built forms, The Design/Planning Dilemma of Courtyards. http://www.new-learn.info/packages/clear/thermal/buildings/configuration/open_spaces_and_built_form/courtyards/images/court_pd.pdf - accessed on September 18, 2015

Mahdavi, A., Kiesel, K., Vuckovic, M. (2014): Empirical and computational assessment of the urban heat island phenomenon and related mitigation measures. Geographia Polonica 87, 505-516

Matzarakis, A., Mayer, H. and Iziomon, M.G. (1999): Applications of a universal thermal index: physiological equivalent temperature. International Journal of Biometeorology 43, 76-84

Meier, A. (1990): Strategic landscaping and air-conditioning savings: A literature review. Energy and Buildings 15, 479-486

Meir, I., Pearlmutter, D. and Etzion, Y. (1995): On the Microclimatic Behavior of Two Semi-Enclosed Attached Courtyards in a Hot Dry Region. Building and Environment 30, 563-572

Met Office. (2011): Microclimates – National Meteorological Library and Archive Factsheet 14. http://www.metoffice.gov.uk/media/pdf/n/9/Fact_sheet_No._14.pdf - accessed on September 18, 2015

Myrup, L. (1969): A numeric Model of the Urban Heat Island. Journal of Applied Meteorology 8, 908-918

Nakayama, T and Fujita, T. (2010): Cooling effect of water-holding pavements made of new materials on water and heat budget in urban areas. Landscape and Urban Planning 96, 57-67

Oke, T.R. (1978): Boundary Layer Climates: 2nd edition, Taylor & Francis Group United Kingdom

Scholz, M. and Grabowiecki, P. (2006): Review of permeable pavement systems. Building and Environment 42, 3830-3836

Shahmohamadi, P., Che-Ani, A., Etessam, I., Maulud, K. and Tawil, N. (2011): Healthy Environment: The Need to Mitigate Urban Heat Island Effects on Human Health. Procedia Engineering 20, 61-70

Steeneveld, G., Koopmans, S., Heusinkveld B., van Hove, L., and Holtslag, A. (2011): Quantifying urban heat island effects and human comfort for cities of variable size and urban morphology in the Netherlands. Journal of Geophysical research 116, D20

Stewart, I. D. & Oke, T.R. (2012): 'Local climate zones' for urban temperature studies. Bull. Amer. Meteor. Soc., 93, 1879-1900

Taha, H., Akbari, H., Rosenfeld, A. and Huang J. (1988): Residential cooling loads and the urban heat island—the effects of albedo. Building and Environment 23, 271-283

Tennis, P., Leming, M. and Akers, D. (2004): Pervious Concrete Pavements. Portlang Cement Association, US

Tsianaka, E. (2006): The role of courtyards in relation to air temperature of urban dwellings in Athens. PLEA2006 – Geneva, Switzerland http://plea-arch.org/ARCHIVE/2006/Vol2/PLEA2006_PAPER173.pdf - accessed on September 18, 2015

Tsutsumi, H., Tanabe, S., Harigaya, J., Iguchi, Y. and Nakamura, G. (2006): Effect of humidity on human comfort and productivity after step changes from warm and humid environment. Waseda University, Tokyo.

University of Gothenburg (2015): Sky View Factor Calculator. http://gvc.gu.se/english/research/climate/urban-climate/software/download – accessed on September 26, 2015

Van Hove, L.W.A., Jacobs, C.M.J., Heusinkveld, B.G., Elbers, J.A., van Driel, B.L. and Holtslag, A.A.M. (2015): Temporal and spatial variability of urban heat island and thermal comfort within the Rotterdam agglomeration. Building and Environment 83, 91-103

Vieira, H. & Vasconcelos, J. (2003): Urban morphology characterization to include in a GIS for climatic pruposes of Libson. Discussion of two different methods.
http://www.ceg.ul.pt/climlis/recent_dev_files/vieira_vasconcelos.pdf - accessed on September 18, 2015

Voogt, J.A. (2004). Urban Heat Islands: Hotter Cities.
http://www.actionbioscience.org/environment/voogt.html - accessed September 18th 2015

WBCSD (2010): Pathways to Energy & Climate Change 2050.
http://www.wbcsd.org/web/publications/pathways.pdf - accessed: Sept. 17, 2015

FIGURES

All other figures made by the author.

APPENDIX

Additional Monitored Data

The data provided in this appendix serves as additional supporting data, which was recorded as part of this thesis but was not used in the main data analysis. The first graph (A1) shows the entire measurement set, which was recorded during the second phase of data collection. This set shows diurnal cycles at 4 different locations between July 7th and July 30th.

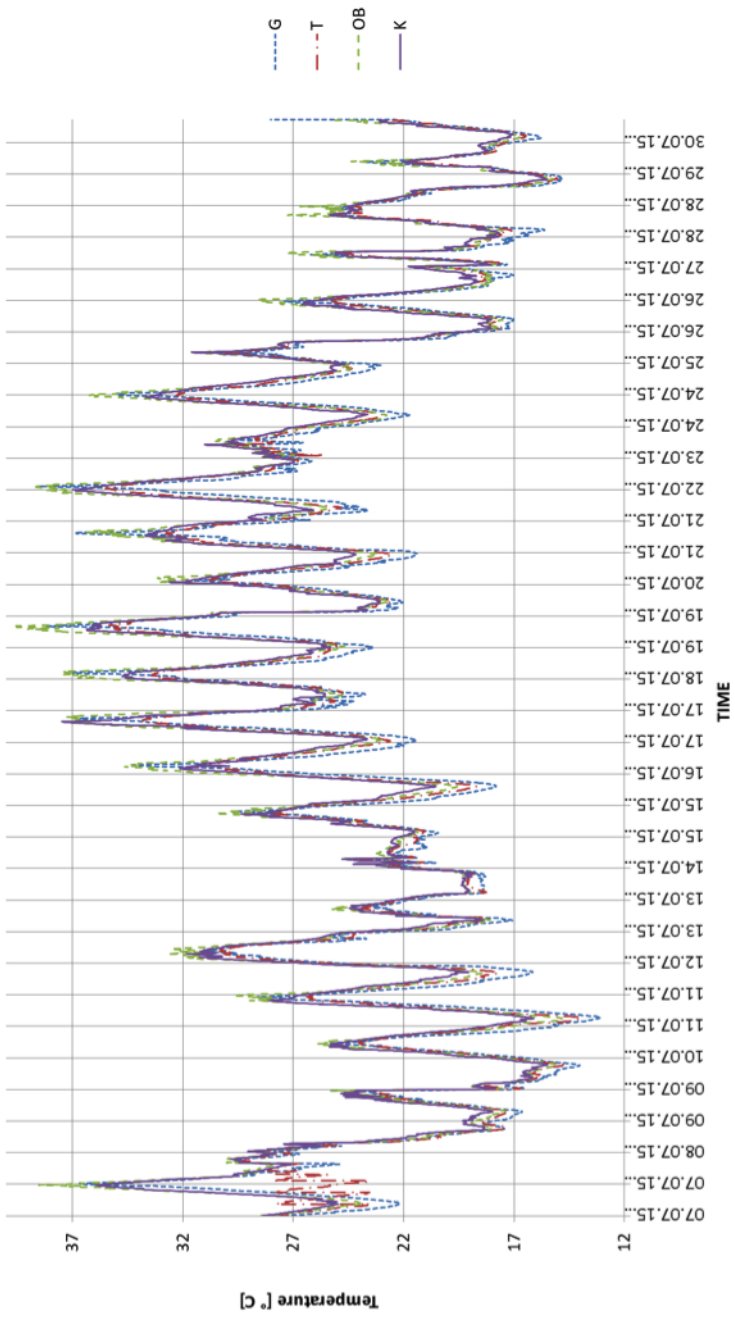

Figure A1: Temperature at 4 courtyards over a period of 3 weeks (July 7th until July 30th 2015)

Figures A2 to A8 are temperature graphs of the remaining 7 locations, which were not shown and discussed in the results and discussion chapters comparing courtyard and street between 13:00 and 17:00. Some graphs are missing several hours of data, because of direct sunlight reaching the temperature sensor and leading to distorted results.

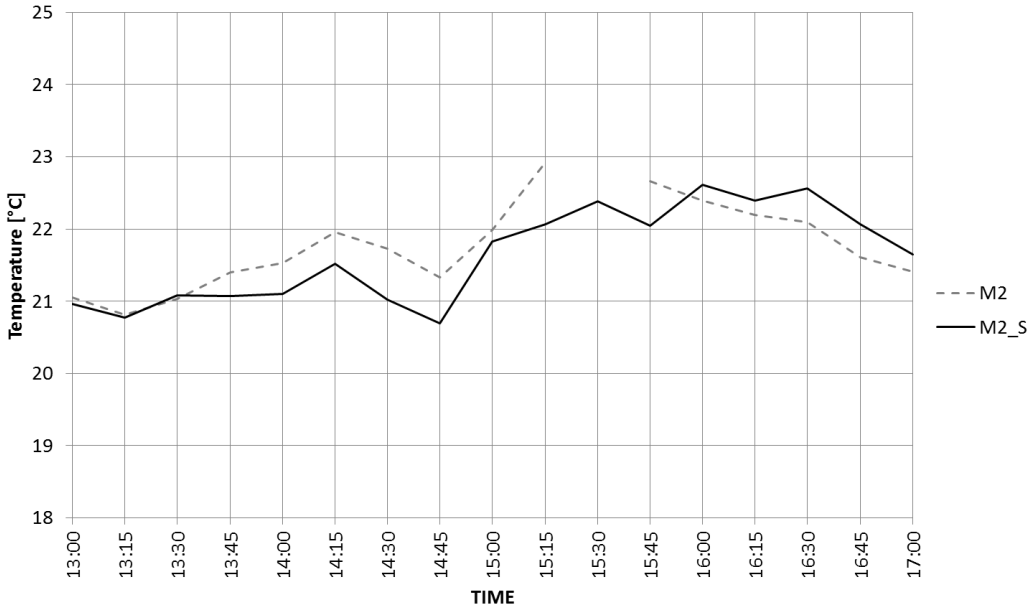

Figure A2: Temperature at courtyard and street (M2) as a function of time of the day measured during afternoon hours (13:00-17:00) on May 7th 2015

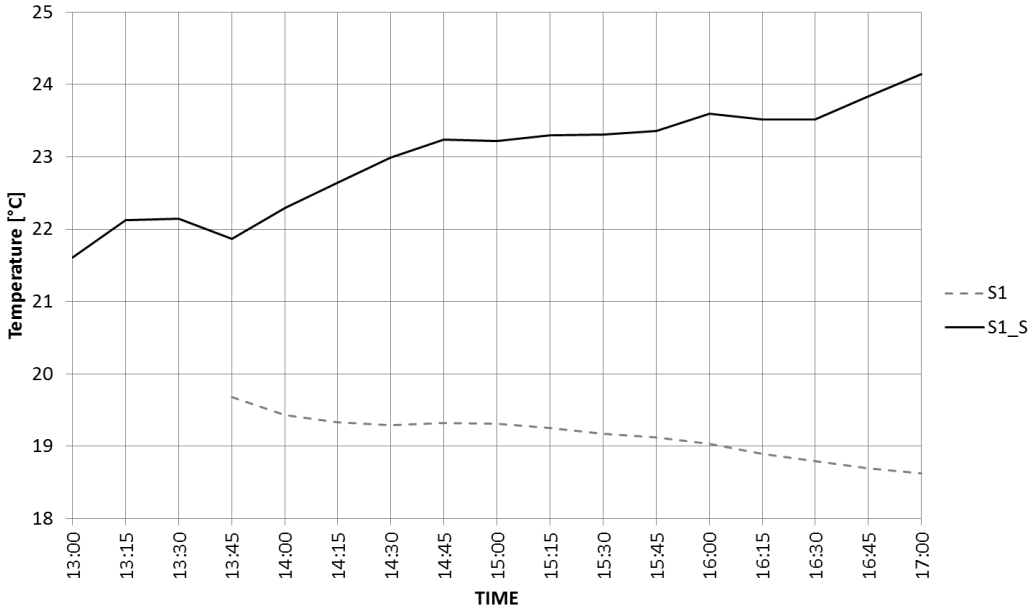

Figure A3: Temperature at courtyard and street (S1) as a function of time of the day measured during afternoon hours (13:00-17:00) on May 8th 2015

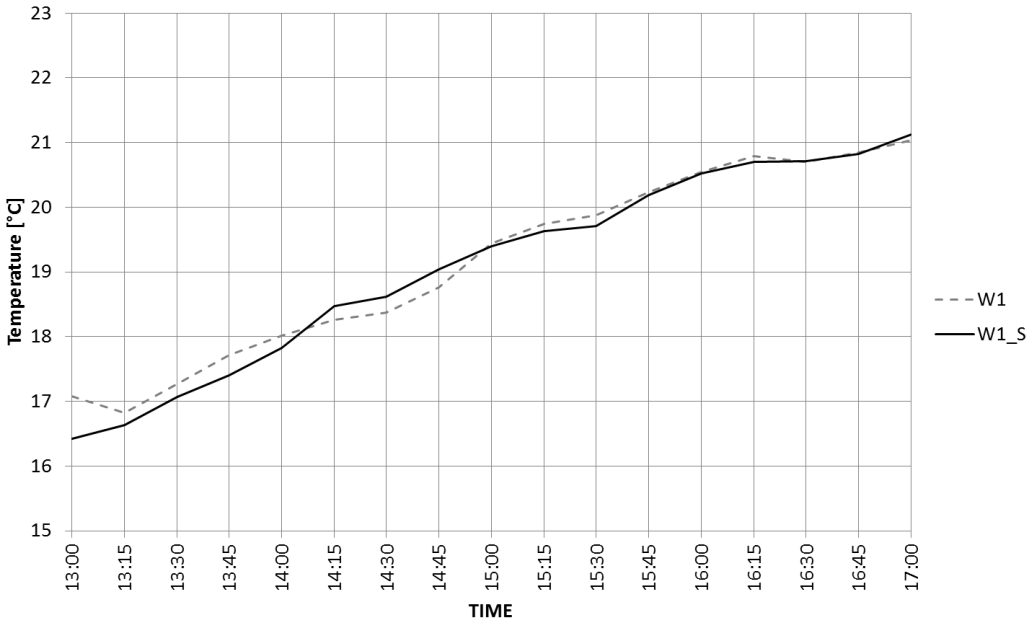

Figure A4: Temperature at courtyard and street (W1) as a function of time of the day measured during afternoon hours (13:00-17:00) on April 23rd 2015

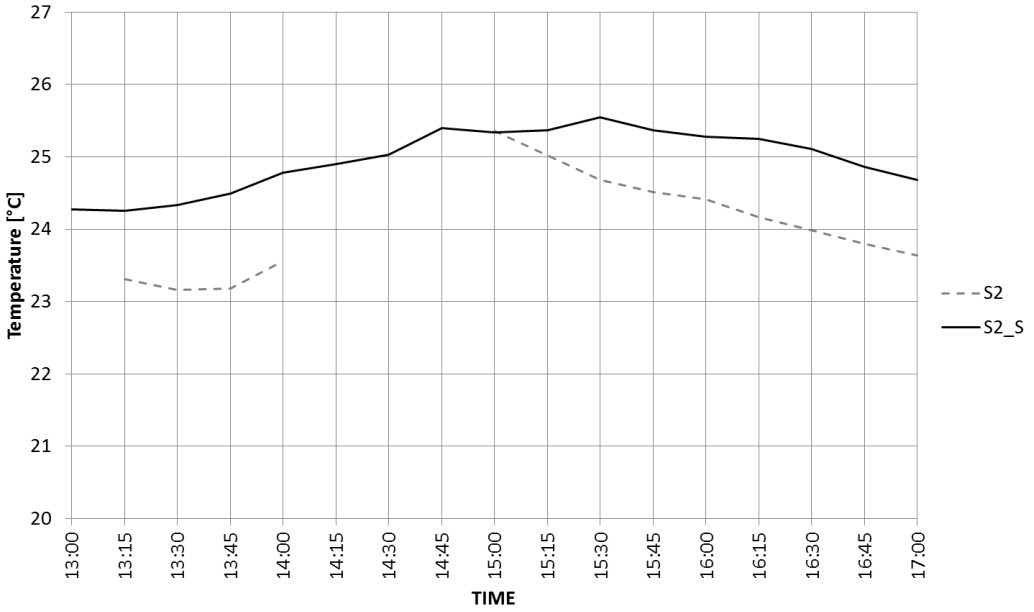

Figure A5: Temperature at courtyard and street (S2) as a function of time of the day measured during afternoon hours (13:00-17:00) on May 12th 2015

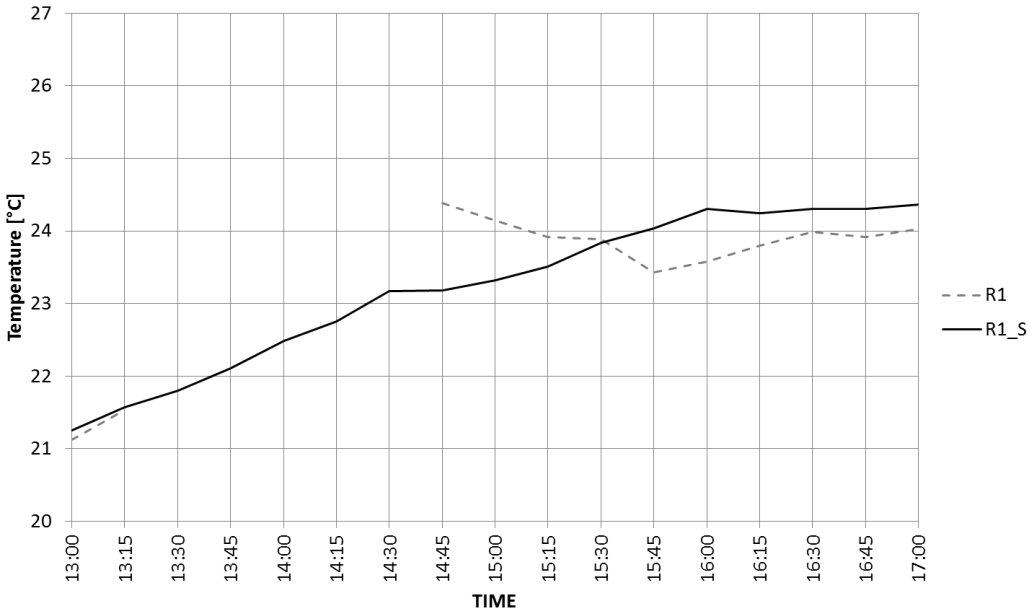

Figure A6: Temperature at courtyard and street (R1) as a function of time of the day measured during afternoon hours (13:00-17:00) on May 18th 2015

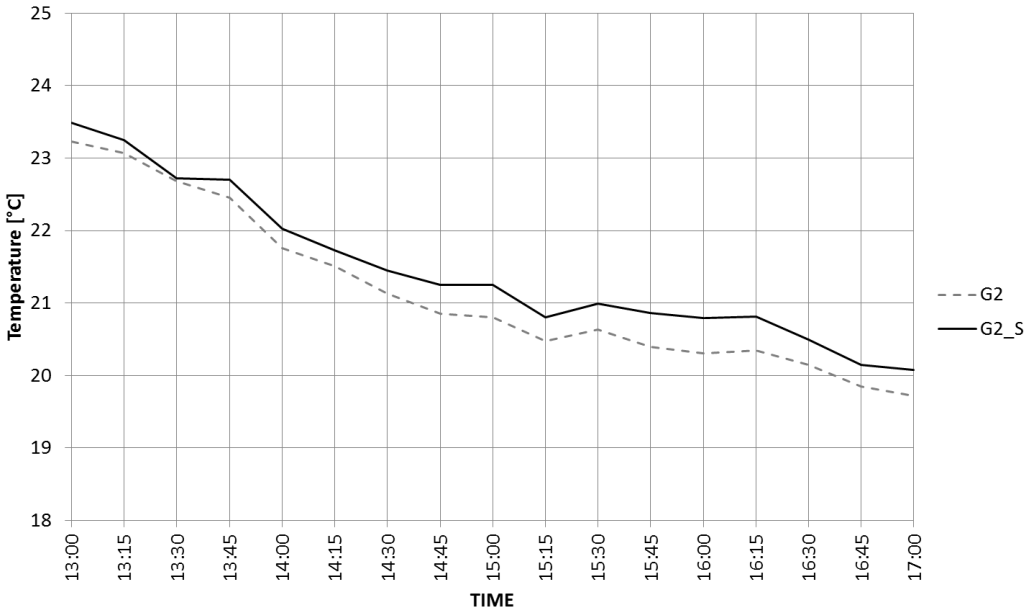

Figure A7: Temperature at courtyard and street (G2) as a function of time of the day measured during afternoon hours (13:00-17:00) on May 19th 2015

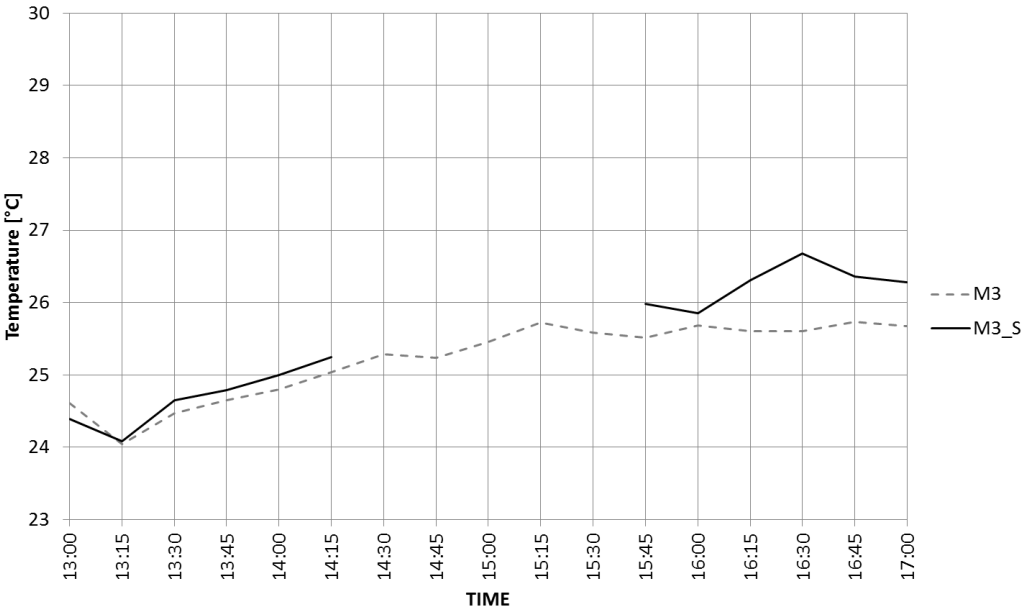

Figure A8: Temperature at courtyard and street (M3) as a function of time of the day measured during afternoon hours (13:00-17:00) on June 5th 2015